On Charge Detection with Inductive Superconducting Single Electron Transistor

M. Sc. Thesis

Jani Tuorila
University of Oulu
Department of Physical Sciences
Theoretical Physics

Oulu 2004

Contents

Preface

Before getting started I would like to thank the persons whose influence have been crucial during the processing of this thesis. First of all, a big thank you to Professor Erkki Thuneberg for instructing and supervising this work. I would also like to thank the whole faculty of Theoretical Physics in the University of Oulu for the great working atmosphere. Especially the guys in room TE319, who were a real cheer-up whenever I needed one. I am extremely grateful to my parents who have always supported me in whatever I have been doing. I would also like to mention the rest of my family, my friends and, particularly, the guys from the football grounds that have constantly reminded me that life is in fact only a small part of football.

Last, and above all, my deepest gratitude goes to my dear wife Sanna, who has been my 'driving force' throughout this year of mental torment.

Oulu, May 24, 2004

Jani Tuorila

Chapter 1

Introduction

"Life is like a box of chocolates. You never know what you're gonna get."
- Forrest Gump

What is the Truth? A Question has been raised and, according to some people's intuition, when that happens there should exist an answer. But is every question *answerable*? Can we tell about the Truth in terms of the *language*? The science fiction novelist T. Pratchett has written in one of his famous *Discworld*-novels that when you remove all that is impossible, you are left with the Truth. But in this way there pops up another question of what is impossible.

Physics is all about the Truth. The experiments made in the laboratories and the everyday observations perceived by our senses tell us bits of the Answer. Conclusions are made based on these discoveries and on the grounds of these conclusions the theories of the Truth are formed. Some of these theories (e.g. quantum theory and theory of relativity) are based on deep thougths about the Universe and the Existence as a whole and *explain* reasonably the observations that have been made. In that way, the theories at issue *describe* the pieces of the Truth that have been detected. However, there is no guarantee that the things we observe are all that *can* be observed. Moreover, it is not certain that everything that can be measured is everything that *is*. Therefore, until it is acceptable to say: "These experiments give us all that is possible, the rest is impossible.", these theories cannot be *called* as the Answer. In this sense the life, and moreover the whole Existence, *is* indeed like a box of chocolates.

One of these observations is the superconductivity. It is a strange phenomenon. First of all, it reveals the peculiarities of the quantum theory on a macroscopic scale [1]. In superconductivity systems of millions of microscopic entities can form up into a single macroscopic quantum system that can excite and tunnel, superpose and entangle. Secondly, it is caused by electrons that, in contrast to our intuition, work in pairs (so called Cooper pairs) [1]. And lastly, there are the numerous phenomena such as the disappearance of electrical resistance at low temperatures, the Meissner effect and the flux quantization that stun by their existence. Altogether, one could say that superconductivity brings out Mother Nature at her best - unpredictable and devious.

It all started in 1911, when the Dutch physicist H. Kamerlingh Onnes discovered that electrical resistance of mercury goes to zero when mercury is cooled below the critical temperature of about 4.2 K. He found out that this critical temperature T_c is a characteristic of a material and is of the order of 1 K to 10 K. Since then many alloys and compounds have been found which have a high critical temperature. Highest to date (2003) is 139 K for Mercury Barium Thallium Copper Oxide or $Hg_{0.2}Tl_{0.8}Ca_2Cu_3O$ [2]. The next milestone was in 1933 when W. Meissner and R. Ochsenweld discovered that the superconducting state is a diamagnetic state. It means that magnetic field is not only excluded from entering a superconductor but also that it is expelled from an originally normal sample when the sample is cooled below T_c. These results tell us that superconductivity is a physical state with zero electrical resistance and zero magnetic field. [3, 4]

The Meissner effect does not occur with arbitrary magnetic fields. In fact, for every superconducting material there exists a temperature dependent critical magnetic field H_c which is strong enough to destroy the zero resistance and take the material back to the normal state. At T_c this field is zero and so there is no Meissner effect at critical temperature. [3, 4, 5]

By the year 1950 these and many more interesting superconductivity related experiments had been performed. All that was missing was the theoretical base which could explain the observed phenomena. In 1950 V. L. Ginzburg and L. D. Landau [6] succeeded in creating a phenomenological theoretical model of the superconductivity. Ginzburg and Landau presumed that there is a complex order parameter that describes the superconducting state. Their discovery was, however, not very much appreciated, until in 1959 and 1960 L. P. Gor'kov was able to show the equivalence between their theory and a theory that was formulated from a microscopic point of view in 1957 [3].

J. Bardeen, L. N. Cooper and J. R. Schrieffer developed this theory (called BCS-theory) [7] and showed that even a weak attractive interaction between electrons is enough to form Cooper pairs. These pairs consist of two electrons which can via the weak atrraction be spread over considerable distances; several pairs can be occupying the same region of space at the same time [1]. As in general, the theoretical basis is needed for the development of superconductivity related applications. Although the theories of superconductivity are rather interesting they itself are not studied a lot farther in this thesis. However, the superconductivity is examined not in general, but concentrating on one of its special applications, namely Josephson junctions.

In 1962 B. D. Josephson [8] was analyzing a situation where two superconducting regions have been connected by a weak insulating layer. He predicted that even when there is no potential difference between the two regions there exists a direct supercurrent through the junction. He also noted that if the two regions are connected to the two terminals of a battery, the current starts to oscillate at high frequency. The Josephson tunneling effect was shown experimentally already in 1963 by P. W Anderson and J. M. Rowell [9] and the oscillations were seen in 1965 by I. K. Yanson et al. [10]. These junctions have numerous applications. For example, two such junctions, when connected in series, can be used in very sensitive charge measurements [1]. If the two junctions are connected in parallel, one has a superconducting quantum interference devices (SQUIDs) which are used, for instance, in qubits which are the building blocks of the quantum computer [11, 12]. They are also very interesting because with them one can display quantum effects on a macroscopic scale.

In his book *Fabric of Reality* [13], David Deutsch has written that the fabric of reality (or the Truth) can be understood only by understanding all the theories that explain it. Because all these theories explain more than can be said out of hand, it is evident that we understand more than we know of. In this thesis the explaining theory is the theory of superconductivity. Even if one understands the whole superconductivity, it is naive to expect that one is therefore able to explain, for example, every single circuit that is made out of superconducting materials. One of these circuits, called the Inductive Single Electron Transistor (L-SET), is presented in this thesis. The L-SET consists of two Josephson tunnel junctions and therefore it is important first to understand the basic ideas of charge tunneling and superconductivity. Tunnel junctions are therefore studied in Chapter 2, in the normal and then in the superconducting

state. The properties of the Josephson junction that are relevant later in the thesis, which include the Josephson effects and the uncertainty relation, are also discussed in detail. A brief introduction to superconductivity is also provided. Also, the effects that are complementary to the usual Josephson ones are discussed.

In Chapter 3 the tunneling rates of a superconducting junction are calculated. The basics of single electron transistors (SET) are also presented. Finally, superconducting SETs are discussed. A peek in quantum computing is also made to get some motivation for the studies of SETs. Chapter 4 is devoted to an introduction of an inductive superconducting SET (L-SET), which is proposed to perform charge measurements near the quantum limit. Classical and quantum mechanical models of the device are formed. Chapter 5 includes the simulations of the dynamics of the system that were made based on the model presented in Chapter 4. Finally, a summary and the conclusions that were drawn are shown in Chapter 6.

Chapter 2

Tunnel Junctions and Superconductivity

"It pleases me as much to doubt as to know."
- Dante Aleghieri

One of the numerous strange phenomena that the quantum theory implies is *quantum tunneling*. What the theory in principle says, is that if one e.g. throws a ball at wall there exists small but altogether definite probability for the ball to go through the wall[1]. The ball is said to tunnel through the wall. Why is it then, that tunneling does not appear in our everyday lives? Why can we not throw a ball through a wall? Why can we not walk through the doors without *opening* them? The explanation lies in our (and the ball's) *macroscopic* nature. Our bodies consist of atoms and, moreover, of elementary particles, such as electrons. Each of these billions of particles has a tiny probability to tunnel through a *potential wall*, let us say a wooden door, for example. Moreover, these particles are coupled with each other so that the probability for all of them to tunnel through becomes negligible.

Although the above discussion is an oversimplification of the things that really happen at microscopic scale, it anyhow gives an idea of the phenomenon of tunneling. In the next few sections this idea is developed by considering two metallic islands that are coupled via thin insulator. In this case the "ball" is an electron and the insulator acts as the "wall". These systems are called *tunnel*

[1]Of course, this does not mean that the ball breaks the wall down. It just goes through it.

junctions. Due to the quantum theory the electrons at both of the conducting islands have finite probabilities of tunneling to the other side of the insulating barrier. If the tunneling events are such that the energy of the electron does not change, the tunneling is called *elastic*.

2.1 Single Tunnel Junction

Let us consider a case with a single tunnel junction. Classically it can be taken as the definition of the capacitor. So, there exists a parameter that characterizes the junction, namely the *capacitance* C. If one considers the junction to consist of two metallic plates separated by an insulator, one gets for the capacitance [14]

$$C = \epsilon\epsilon_0 \frac{A}{d}, \tag{2.1}$$

where ϵ is the electric permittivity of the insulator, ϵ_0 is the permittivity of the free space, A is the area of a plate and d is the thickness of the insulator. This is a very good approximation [15] even in small sizes. If a constant potential difference (with a battery with voltage V) is produced accross the junction, the plates are charged with equal but opposite charges. Effectively, the battery *transfers* the charge from one plate to another. The potential of a plate is the same as the potential of the terminal of the battery it is connected to. Therefore the potential difference between the junction plates is the same as that of the terminals of the battery. If the battery is disconnected the charge remains on the plates by the mutual attraction (in the classcical picture of the junction). The magnitude of the charge Q of the plates is directly proportional to the voltage V, i.e.

$$Q = CV, \tag{2.2}$$

where the capacitance C can be thought to be determined by the *geometrical* properties of the junction[2], i.e. A and d. The potential energy of a capacitor is the amount of work the battery has to do to charge the capacitor. The work needed to transfer an infinitesimal charge dq from one plate to another is $dW = Vdq = (q/C)dq$. The total work done to charge the capacitor is therefore [14]

$$U = \int_0^Q \frac{q}{C} dq = \frac{Q^2}{2C}. \tag{2.3}$$

[2]That is, when the insulating material, that sets the ϵ, has been chosen.

This is the *electrical potential energy* of the capacitor.

This picture alters a little when one takes the quantum effects into consideration. Because of the possibility of electron tunneling through the junction there exists a small leakage current. With small potential differences the current-voltage relationship of the junction can be taken *linear*, which defines the tunneling resistance R_T. The tunnel junction can therefore be modelled by a capacitor with capacitance C and a resistor with resistance R_T connected parallel. If one disconnects the battery, the capacitor starts to act as a voltage source and the energy stored in it dissipates as heat in the resistor.

The knowledge obtained from the quantum theory tells that the charge is a quantized concept. The smallest amount of charge that exists free in the nature is the charge of an *electron*. However, because of the continuous nature of the voltage V, the junction can be charged to any charge, even to the fractions of the charge of an electron. This is due to a fractional shift of the electrons in the junction plates with respect to the positive ionic background. On the other hand, the tunneling events concern only a discrete change of charge. In the following, the single electron tunneling effects are considered.

2.1.1 Ultra Small Tunnel Junction

As can be seen in Equation (2.1) the capacitance of a tunnel junction is dependent on its dimensions. So, the smaller the capacitor is, the smaller is the capacitance. This means, according to Equation (2.3), that the potential energy stored in a capacitor gets bigger as the dimensions of the capacitor get smaller[3], assuming the charge on the plates is kept constant. When the capacitor is small enough the behaviour of a single electron becomes important.

Before that can happen, two conditions have to be fulfilled. Firstly, the charging energy of a single electron, $E_c = e^2/2C$, has to be substantially larger than the average thermal energy k_BT (k_B is the Boltzmann's constant, T is the temperature), i.e.

$$E_c \gg k_BT. \tag{2.4}$$

This ensures that the single electron charging effects are not smeared out by *thermal fluctuations*. The condition (2.4) means that for $T \sim 1$ K the capacitance of the junction has to be smaller than 10^{-15} F. Secondly, the

[3]This is the case also when one takes the quantum effects into account. It only takes a little bit of extra work for the battery to heat up the resistive channel of the junction.

charging energy of a single electron must be larger than quantum uncertainty of energy

$$E_c \gg \Delta E \geq \hbar/\Delta t. \tag{2.5}$$

Here the $\hbar$ is the Planck's constant divided by 2π and Δt is the finite lifetime of the charge on the capacitor plate. This lifetime can be approximated with the time constant $\tau = R_T C$, which is the charge relaxation time. This means in practice, that the charge on the capacitor plates is assumed to resume equilibrium before the next tunneling event can occur. So, one gets

$$E_c = \frac{e^2}{2C} \gg \frac{\hbar}{R_T C} \Rightarrow R_T \gg \frac{2\hbar}{e^2} \approx R_Q. \tag{2.6}$$

Here the $R_Q = \hbar/e^2$ is the so called *resistance quantum*. The condition

$$R_T \gg R_Q \tag{2.7}$$

ensures that the wave function of the charge carrier on a junction plate is localized there. This means that under condition (2.7) the single electron charging effects are *not* washed away by *quantum fluctuations*.

But what are these single electron charging effects? This question is answered in the following chapter, but at first, tunnel junctions with superconducting plates are considered.

2.2 Superconductivity and Josephson Junctions

Before proceeding to the superconconducting tunnel junctions, a few words about the basic phenomenom of superconductivity are discussed. As mentioned in the Introduction, superconductivity is a physical state that exists when the temperature and the magnitude of the external magnetic field are below their critical values. These values are characteristic to the material at hand. The effects of this state were mentioned to be the infinite conductance, the Meissner effect etc. But what is the explanation that lies behind these observations? Why do some materials become superconductive in right circumstances? Qualitatively superconductivity can be understood like this. Let us take two electrons that are in the superconducting material. Intuitively one considers that, like in a vacuum, these electrons repell each other due to the Coulomb interaction. But, however, the situation is now different from that in an empty space. The electrons are located in a *medium*, i.e. in the crystal,

and this, in fact, can change the sign of their interaction. Namely, when an electron is moving in a superconducting material it deforms the crystal lattice by means of electric forces. This displacement of the ions in the lattice affects the state of the other electron, which sees a somewhat altered structure of the polarized lattice. As a result the electron is surrounded by a "cloud" of positive charge. This cloud is attracted to a single electron and the magnitude of the charge of this positive cloud can exceed the charge of an electron. So, one of our electrons together with the positive cloud can have positive net charge and therefore might be able[4] to be attracted by the other one. At high temperatures the thermal oscillations wash away these effects, but at low temperatures they are of great importance. [16]

Based on the above discussion, the electrons might be able to exist in *pairs*. These electron-electron pairs are called *Cooper pairs*. This is a crude way of describing things, because, for example, it is possible for two pairs to occupy the same region of space at same time. It is, however, a sufficient way for the purpose of this thesis.

But how do these Cooper pairs explain the superconductivity? The answer lies in the spin of a Cooper pair. A single electron is a *fermion*. This means, that it follows the Pauli's exclusion principle, which says that no two identical particles can be in the same physical state at the same time. A Cooper pair, however, is not a fermion. It consists of two fermions and is therefore a *boson*. The bosons do not follow Pauli's principle. Quite on the contrary, when there are many bosons in a given state there is an especially large probability for the others to go to the same state [1]. This way one could describe the state of a superconductor by a single wave function that describes the behaviour of the whole electron system as a unit. As can be noted from above, all the Cooper pairs in a superconductor are in a common physical state and therefore have the same energy. Moreover, a finite energy must be expended, if one wants to excite this state. This common state is referred to the *ground state* of the superconductor and the Cooper pairs are said to form a *condensate*. The finite energy difference that is between the ground state and the excited state is called the *energy gap* and denoted by Δ. The excitation of the system can be described as a breakup of a Cooper pair and the energy needed for such an operation is 2Δ, which is the so called *pair binding energy*. For example, the absence of the electrical resistance of the superconductors can be explained by energy gap. That is, because it is known that the electrical resistance of a

[4]I.e. it is not prohibited by the laws of physics we know of.

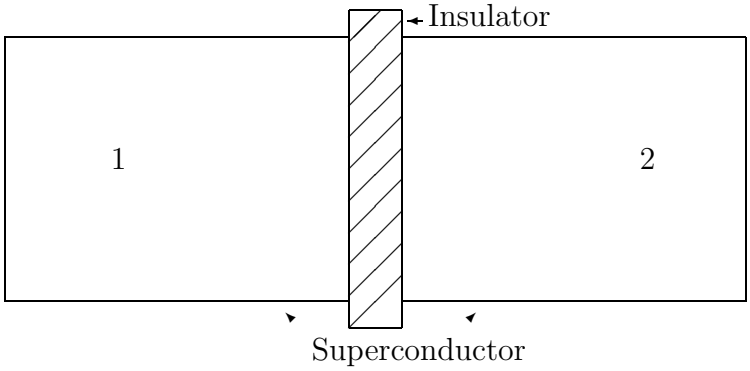

Figure 2.1: Two superconductors coupled with thin insulator.

metal is due to the interaction between the moving electron system (that is, the electric current) and the vibrations of the lattice or with impurities. Due to the energy gap, however, these quantum transitions will not always be possible. This implies, that the electron system will not be excited when it is moving slowly. It means, that the charge transfer is frictionless, i.e. no electrical resistance occurs. This way of thinking also defines the *critical current*. When this current is exceeded the superconductivity disappears. [16]

The most astonishing thing about this way of explaining the superconductivity is the existence of the superconducting gap. It means that the energy spectrum of the common wave function is discrete. This tells us, that a superconductor, that is described by millions of Cooper pairs that form a single entity, is actually a *Macroscopic Quantum Object*.

These ideas are the basis of the theories that explain the superconductivity, for example the BCS- and the GL-theories. However, some people may say that this way of explaining the superconductivity only leads us to a new problem: How to determine exactly the electron-electron attraction? Some of them may even ditch the theory on the grounds of this question. But, all in all, especially to those people: This possible attraction is not prohibited by the laws of physics known to us. Moreover, it explains the phenomenon, and actually is the best explanation that we have. Therefore, until a better theory is needed and provided, one should be content with this one.

a) *b)*

Figure 2.2: Symbol for a a) normal metal tunnel junction and b) superconducting tunnel junction.

Josephson Junction

As mentioned in the Introduction a Josephson junction consists of two superconducting regions that are coupled via a thin insulator (see Figure 2.1). Circuit symbols for normal metal and superconducting tunnel junctions are presented in Figure 2.2. The insulating layer must be thin enough so that the probability for the electrons to tunnel through becomes sufficiently large. If one thinks the junction classically one notices that it is like an ordinary capacitor with a characteristic capacitance C [17]. By connecting the junction to an external circuit one finds out that it may be charged with a charge $Q = CV$ where V is the voltage across the junction [17]. Similarly, as discussed in the previous section dealing with tunnel junction in general, the voltage V is a continuos variable and therefore the junction charge Q can be continuously polarized, with respect to the positive background of ions of the junction plates, even on the scale of an elementary charge. When the quantum effects are taken into account it is possible that charge is transported through the insulating barrier. In the superconducting state the tunneling particles are Cooper pairs and so the transported charge is $2e$. This type of transport involves only discrete changes of charge and a typical change of energy for the process is the charging energy $E_c = (2e)^2/2C$, where e is the elementary charge [17].

Because a Josephson junction consists of two superconductors, such as in the Figure 2.1, it must be cooled down below the critical temperature T_c for the two superconducting regions to be in the superconducting state. This is necessary to see the superconducting effects, i.e. the Cooper pair tunneling. If the junction is in high temperatures, i.e. above T_c, it acts just as a normal metal tunnel junction. For the reasons presented above, as the temparture falls the electrons try to reach the energetically lowest state which leads to formation of Cooper pairs. These pairs are expected to be moving in the

same state. In this state both sides 1 and 2 of Fig. 2.1 are characterized by Ginzburg-Landau (GL) order parameters Ψ_1 and Ψ_2, respectively [5]. Let us call these order parameters the common wave functions of pairs and write them as [1]:

$$\begin{aligned} \Psi_1 &= \sqrt{\rho_1} e^{i\theta_1}, \\ \Psi_2 &= \sqrt{\rho_2} e^{i\theta_2}, \end{aligned} \tag{2.8}$$

where ρ_1 and ρ_2 are the densities of electrons on the two sides of the junction and θ_1 and θ_2 are the phases of the wave functions at those sides.

2.2.1 Josephson Effects

The discussion in this subsection is based on Reference [1]. Let us now think that the junction is symmetrical, i.e. the superconducting material is the same on the both sides of the insulator. In the following it is also assumed that there exists no magnetic field. Then the equations for two weakly coupled superconductors are the standard equations for two coupled quantum mechanical states

$$\begin{aligned} i\hbar \frac{\partial \Psi_1}{\partial t} &= U_1 \Psi_1 + K \Psi_2 \\ i\hbar \frac{\partial \Psi_2}{\partial t} &= U_2 \Psi_2 + K \Psi_1, \end{aligned} \tag{2.9}$$

where the constant K is a characteristic of the junction and $\hbar$ is Planck's constant divided by 2π. If K were zero then there would be no coupling and the equations would describe the lowest energy state of each superconductor, with corresponding energy U. But, due to the coupling, the K-factor is non-zero and there can be some leakage from one side to the other. Now, if there is a potential difference V across the junction, then U_1 and U_2 are not equal, but $U_1 - U_2 = qV$, where q is the charge of a pair. If the zero of energy is defined halfway between them, the coupled equations are

$$\begin{aligned} i\hbar \frac{\partial \Psi_1}{\partial t} &= \frac{qV}{2} \Psi_1 + K \Psi_2, \\ i\hbar \frac{\partial \Psi_2}{\partial t} &= -\frac{qV}{2} \Psi_2 + K \Psi_1. \end{aligned} \tag{2.10}$$

Let us substitute Ψ_1 and Ψ_2 by the ones defined in Equation (2.8). Moreover, $\rho_{1,2}$ and $\theta_{1,2}$ are the electron densities and the phases of the wavefunctions on

the two sides of the junction, respectively. One should note that in practice the electron densities are almost exactly equal to the normal density of electrons ρ_0 in the superconducting material. This way one arrives at

$$\begin{aligned}
\dot{\rho_1} &= \frac{2}{\hbar} K \sqrt{\rho_1 \rho_2} \sin \Delta\theta, \\
\dot{\rho_2} &= -\frac{2}{\hbar} K \sqrt{\rho_1 \rho_2} \sin \Delta\theta, \qquad (2.11) \\
\dot{\theta_1} &= \frac{K}{\hbar} \sqrt{\frac{\rho_2}{\rho_1}} \cos \Delta\theta - \frac{qV}{2\hbar}, \\
\dot{\theta_2} &= \frac{K}{\hbar} \sqrt{\frac{\rho_1}{\rho_2}} \cos \Delta\theta + \frac{qV}{2\hbar}. \qquad (2.12)
\end{aligned}$$

Here $\Delta\theta = \theta_2 - \theta_1$. As justified in Reference [1], one can write, how the current would start to flow from side 1 to side 2. According to Equation (2.11) this current is of form

$$I = \frac{2K}{\hbar} \sqrt{\rho_1 \rho_2} \sin \Delta\theta. \qquad (2.13)$$

Because the junction is connected to a battery, the charge densities do not change and the current can be written as in Equation (2.13). In fact, the charge densities can be written as equal to ρ_0, and then we can set $2K\rho_0/\hbar = I_c$, which leads to the so-called *DC Josephson effect*

$$I = I_c \sin \Delta\theta. \qquad (2.14)$$

I_c is the critical current of the junction. It is the maximum supercurrent the junction can support and, like K, a number that is a characteristic of the junction. [1, 3]

Gauge-invariant Phase

The above discussion has been carried out in terms of the phase difference $\Delta\theta$. Because it is not a gauge-invariant quantity it cannot in general determine the current I, which is a well-defined gauge-invariant physical quantity. The problem is solved by introducing the gauge-invariant phase difference:

$$\varphi \equiv \Delta\theta - (2\pi/\Phi_0) \int \mathbf{A} \cdot d\mathbf{s}, \qquad (2.15)$$

where $\Phi_0 = h/2e$ is the magnetic flux quantum and $\mathbf{A}$ is the vector potential. By replacing $\Delta\theta$ in Equation (2.14) by φ one gets the general expression for

the supercurrent in an ideal Josephson junction:

$$I = I_c \sin \varphi \tag{2.16}$$

This means that if there is no magnetic field present, $\Delta\theta$ and φ can be used interchangably. [3]

Ac Josephson Effect

The pair of Equations (2.12) tells us that (when no magnetic field is present)

$$\dot{\varphi} = \Delta\dot{\theta} = \dot{\theta}_2 - \dot{\theta}_1 = \frac{qV}{\hbar}. \tag{2.17}$$

It is worthwhile to remember, that q is the charge of a pair which is equal to $2e$. Therefore,

$$\dot{\varphi} = \frac{2eV}{\hbar}, \tag{2.18}$$

which is called the *AC Josephson effect*.

So, if the junction is connected to a constant voltage V the Cooper pairs should gain the energy $2eV$ when tunneling through the insulator. In normal metal tunnel junctions part of the energy is dissipated via the resistive channel of the normal tunnel junction, as was seen previously. In Josephson junctions this is not the case. Instead, the energy acquired by the Cooper pair is not needed to overcome the resistance but is radiated away as a light quantum of frequency $2eV/\hbar$. This radiation can be and has been observed experimentally. These experiments show that the electrons indeed work in pairs. [16]

Together with relation (2.14) one gets that if the junction is connected to a dc voltage source the current oscillates like the sine function. These are the so-called *Josephson oscillations*. There exist no net current through the junction on the average. But at zero voltage one gets a current that can be of any amount between $-I_c$ and I_c depending on the phase difference across the junction [1].

Josephson Energy

Josephson relations (2.14) and (2.18) can be used to show that energy can be stored in the Josephson junction. This is seen if one calculates the work done by the external voltage source in changing the phase difference, i.e.

$$W = \int IV\, dt. \tag{2.19}$$

By substituting $I = I_c \sin\varphi$ and $\dot{\varphi} = 2eV/\hbar$, one arrives at the relation

$$W = C - E_J \cos\varphi, \tag{2.20}$$

where C is an integration constant and $E_J \equiv \hbar I_c/2e$. The integration constant C is determined by the choice of the zero level of energy. Then, the energy (where the zero level of energy has been chosen so that $C \equiv 0$)

$$U_J(\varphi) = W = -E_J \cos\varphi \tag{2.21}$$

can be taken as the "potential" energy of the supercurrent I. E_J is the so-called *Josephson energy*.

Previously two important energy scales, considering the effects in ultrasmall tunnel junctions, were discussed. These were the charging energy $E_c = e^2/2C$ related to a situation where a single electron tunnels, and the thermal energy k_BT that causes the thermal fluctuations. In addition to these, the Josephson energy of a junction is also of great importance when determining the dynamics of the junction. If the charging energy of the junction is much larger than the Josephson coupling energy ($E_c >> E_J$) then, due to the quantum nature of the phase charge relationship (as will be shown in the following), the charge is a well defined quantity and fluctuates only little. This is called the *weak coupling regime*. On the other hand, if the Josephson coupling energy is much larger than the charging energy ($E_J >> E_c$) then the phase is well defined and does not fluctuate. This is called the *strong coupling regime*. The effects of these regimes are discussed later in this section. [17]

2.2.2 Quasiparticles and the RCSJ Model

All the discussion presented above have neglected one important aspect. That is, that the *absolute zero* temperature cannot be achieved. This means, that no matter how much the Josephson junction is cooled, there still exists a small but finite temperature T that gives rise to a nonvanishing thermal energy k_BT. This energy is able to break some of the Cooper pairs in the condensate creating single "normal" electrons. The quotes are used with the word normal because the presence of the condensate makes the properties of these electrons different from those in a normal metal. Therefore they are often called as *quasielectrons* or *quasiparticles*.

When the voltage $V = 0$ across the junction, these quasiparticles do not contribute to the current. This is due to their normal electron properties, i.e.

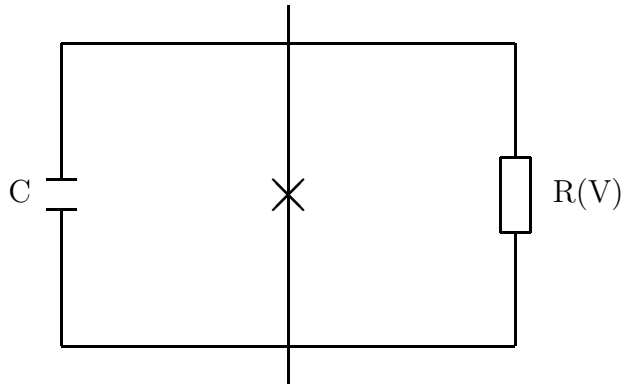

Figure 2.3: The equivalent circuit of the RCSJ model.

they do not form a condensate and therefore cannot present any superconducting properties. But, if voltage $V \neq 0$, the quasiparticles *can* contribute to the current. This defines, as in normal metal junctions, the tunneling resistance R for the quasiparticles. It should be noted that there still exists no resistance for the Cooper pair current. In addition the junction is always characterized by the capacitance C between the two superconducting plates. Therefore, the finite voltage situations can be modelled by an ideal Josephson junction shunted by a resistance R and capacitance C(see Figure 2.3). This model is called the resistively and capacitively shunted junction (RCSJ) model. [3] Because the pair binding energy is 2Δ, high enough voltages, $V > V_g \equiv 2\Delta/e$, can also break Cooper pairs. In this case the tunneling resistance is of the order of the normal state tunneling resistance R_T. On the other hand, if $V < V_g$ and, of course, $T < T_c$, the R is approximately $R_T e^{\Delta/k_B T}$. [3]

The time dependence of the phase φ in the RCSJ model can be derived in the presence of an externally supplied bias current I. This is done by equating I to the total junction current through the three parallel channels [3]

$$I = I_c \sin\varphi + V/R + C dV/dt. \tag{2.22}$$

The voltage V can be written in terms of φ which implies

$$d^2\varphi/d\tau^2 + Q^{-1}d\varphi/d\tau + \sin\varphi = I/I_c \tag{2.23}$$

where a dimensioless time variable $\tau = \omega_p t$ is introduced, with

$$\omega_p = (2eI_c/\hbar C)^{1/2} = (8E_J E_c)^{1/2}/\hbar \tag{2.24}$$

being the so-called plasma frequency of the junction. The *quality factor* Q is defined by

$$Q = \omega_p RC. \tag{2.25}$$

Q^2 is identical to the damping parameter β_c, which was introduced by W. C. Stewart and D. E. McCumber [18, 19] . When $Q < 1$ one has an overdamped junction and if $Q > 1$ an underdamped one [3].

Equation (2.23) is the *equation of motion* of the RCSJ-system. It can be rewritten as

$$E_J d^2\varphi/d\tau^2 + E_J Q^{-1}d\varphi/d\tau + \frac{d}{d\varphi}\big[-E_J\cos\varphi - (I\hbar/2e)\varphi\big] = 0, \tag{2.26}$$

where the relation $I_c = (2e/\hbar)E_J$ has been used. Classically, the equation of motion gives the time development, i.e. the dynamics, of the system. The first term on the left hand side of Equation (2.26) can be thought to be some kind of consequence of the kinetic energy of the system. The third term is due to the potential energy. If the second term, describing the dissipation to the environment, is disregarded, the equation of motion can be thought to be derived from the *Lagrangian* $\mathcal{L}$ of the system. The Lagrangian is the difference between the kinetic and the potential energies of the system. The derivation is done with the help of *Lagrange's equations* [20]

$$\frac{d}{dt}\left(\frac{\partial\mathcal{L}}{\partial\dot{q}_i}\right) - \frac{\partial\mathcal{L}}{\partial q_i} = 0, \tag{2.27}$$

where the q_i's and $\dot{q}_i$'s are the generalized coordinates and velocities of the system, respectively. The maximum value of i is the number of equations. This maximum value is set by the number of degrees of freedom. In Equation (2.23) the generalized coordinate is $\hbar\varphi/2e$. The Lagrangian $\mathcal{L}$ describing the RCSJ-system is taken to be such that its kinetic energy depends only on second power of the generalized velocity and its potential energy is dependent only

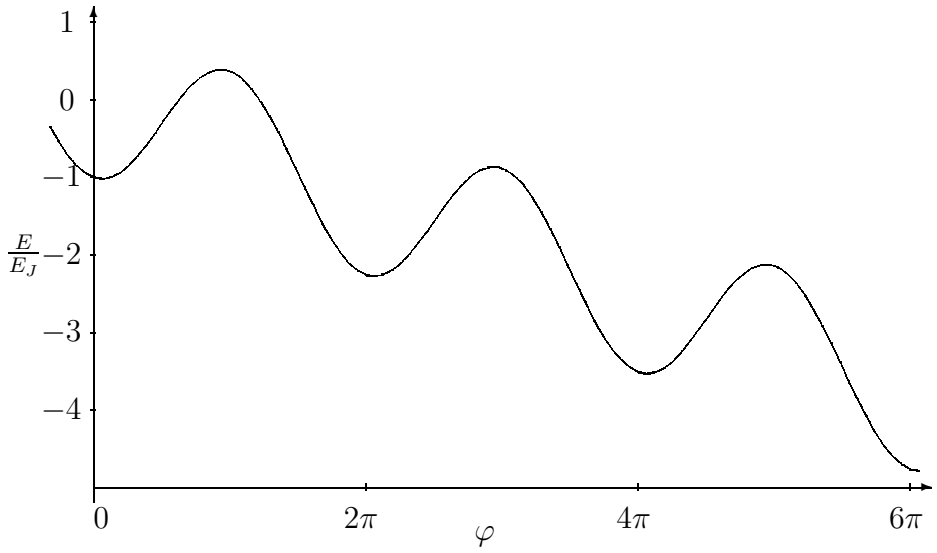

Figure 2.4: The tilted-washboard potential.

on the generalized coordinate. Thus, the term $-E_J \cos\varphi - (I\hbar/2e)\varphi$ can be taken as the potential energy of the system and it is denoted by

$$U_J(\varphi) = -E_J \cos\varphi - (I\hbar/2e)\varphi. \tag{2.28}$$

This is the so called "tilted washboard" potential, which can be seen in Figure 2.4. It has a mechanical analog described in Reference [3] pp. 204-205. The state of the system at low biasing currents (i.e. $I < I_c$) is obtained by minimizing the energy by a classically well-defined value of φ at the minimum of a well of the tilted cosine potential [21]. In this limit the total Hamiltonian of the junction can be written as

$$\mathcal{H} = \frac{Q^2}{2C} - E_J \cos\varphi \approx \frac{Q^2}{2C} + \frac{1}{2}E_J\varphi^2 - E_J. \tag{2.29}$$

Here the deviation from the minimum of the potential well has been taken to be small. One can neglect the constant E_J in Equation (2.29) by setting zero level of energy at $-E_J$. With small phases, the supercurrent $I = I_c \sin\varphi \approx I_c\varphi$, and so one gets

$$\mathcal{H} = \frac{Q^2}{2C} + \frac{E_J I^2}{2I_c^2} = \frac{Q^2}{2C} + \frac{L_J I^2}{2}, \tag{2.30}$$

where it has been denoted $L_J = E_J/I_c^2$. The L_J defines the *inductance* of the Josephson junction. This way one sees that when the phase is localized

in one of the minima of the potential and fluctuates only little, the system behaves like an LC-circuit, where the charge oscillates. These circuits behave like harmonic oscillators, as is known from the basic electrodynamics. So, the energy states of the phase of the Josephson junction are the well known states of the harmonic oscillator. The frequency of this oscillation is the usual $\omega = 1/\sqrt{L_J C} = \sqrt{8E_J E_c}/\hbar$. This frequency is naturally the same as the plasma frequency defined by Equation (2.24). This way one gets a qualitative picture of the dc Josephson effect.

If the biasing current is grown high enough (i.e. $I > I_c$), the phase is able to escape from the potential minimum and as a consequence the current starts to oscillate according to the ac Josephson relation (2.18). Moreover, no current can be detected on average, as discussed in the previous subsection.

2.2.3 Quantum Picture of the Junction

If one wants to analyze the so called secondary quantum effects (tunneling and interference) in the Josephson junction one should consider all the quantities describing the junction as quantum mechanical operators rather than classical variables [22]. The operators that correspond to the main variables, the phase difference φ and the electric charge Q of capacitance C of the junction, satisfy the commutation relation [22]:

$$[\check{\varphi}, \check{Q}] = 2ei. \tag{2.31}$$

This can be easily derived starting from the charging energy

$$E_Q = \frac{1}{2}CV^2 = \frac{1}{2}C\left(\frac{\hbar}{2e}\right)^2 \dot{\varphi}^2. \tag{2.32}$$

This can be taken as some kind of kinetic energy when the corresponding potential energy is the Josephson coupling energy $U_J = -E_J \cos\varphi$. Now the Lagrangian of the system is

$$\mathcal{L} = \frac{1}{2}C\left(\frac{\hbar}{2e}\right)^2 \dot{\varphi}^2 + E_J \cos\varphi. \tag{2.33}$$

From the Lagrangian one can get the generalized momentum [23]:

$$p = \frac{\partial \mathcal{L}}{\partial \frac{\hbar}{2e}\dot{\varphi}} = C\frac{\hbar}{2e}\dot{\varphi} = CV = Q. \tag{2.34}$$

Now the commutation rule for the canonical variables is

$$[\check{x}, \check{p}] = i\hbar, \tag{2.35}$$

so that

$$[\check{\varphi}, \check{Q}] = 2ei. \tag{2.36}$$

From this commutator relation we get the Heisenberg's uncertainty relation for $\check{\varphi}$ and $\check{Q}$. It also gives that

$$\check{Q} = \frac{2e}{i}\frac{\partial}{\partial\varphi}. \tag{2.37}$$

2.2.4 Quasicharge and the Bloch-Wave Oscillations

Using the consepts of the previous subsection, one gets the Hamiltonian function of a Josephson junction in its simplest form

$$\mathcal{H} = \frac{Q^2}{2C} - E_J \sin\varphi = -\left(E_c \frac{\partial^2}{\partial(\varphi/2)^2} + E_J \cos\varphi\right). \tag{2.38}$$

This Hamiltonian describes the sum between the "kinetic energy" $E_c = Q^2/2C$ and the "potential" energy $U_J = -E_J \sin\varphi$ of the junction. The most important thing in this Hamiltonian is that even though the potential is periodic in φ, the states of the Josephson junction before and after a 2π translation of the phase φ are, nevertheless, distinguishable [22]. This implies that the Hamiltonian (2.38) is similar to the Hamiltonian of a one-dimensional quantum particle of mass $(\hbar/2e)^2 C$ moving with momentum $(\hbar/2e)Q$ along the φ axis in a periodic field of the potential $F_J(\varphi)$ [22]. The situation therefore resembles that of mutually noninteracting electrons in periodic potential of an ionic lattice. This analogy can be used as long as the energy dissipation is disregarded. The wave function of the Hamiltonian (2.38) should analogously consist of Bloch waves [22]

$$\begin{aligned} &\Psi(\varphi) = \sum_s \int dk C_k^{(s)} \Psi_k^{(s)}, \quad \Psi_k^{(s)} = u_k^{(s)}(\varphi)\exp(ik\varphi) \\ &u_k^{(s)}(\varphi + 2\pi) = u_k^{(s)}(\varphi), \quad s = 0, 1, 2, \ldots, -\infty < k < \infty \end{aligned} \tag{2.39}$$

Sometimes the variable

$$q = 2ek \tag{2.40}$$

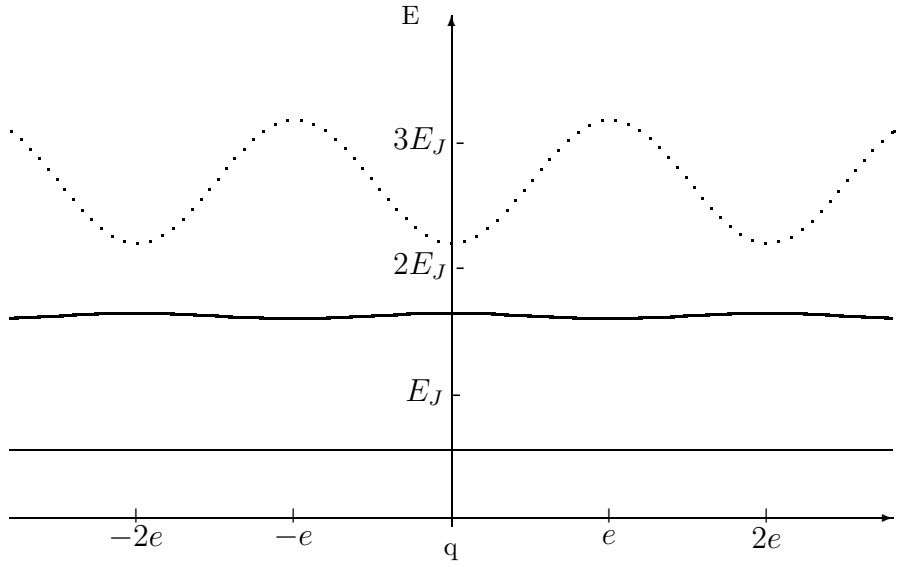

Figure 2.5: Dispersion curves of the energy bands of the Hamiltonian (2.38) with with ratio $E_c/E_J = 0.14$.

is used to give the wave number k the dimension of the electric charge. This variable differs from the real charge Q to the extent that the quasimomentum of an electron in a crystal lattice differs from its real momentum [22]. That is why q is called the *quasicharge*.

If one writes down the Schrödinger equation for such a Hamiltonian, one gets the Mathieu equation

$$\mathcal{H}\Psi = E\Psi \Rightarrow \frac{\partial^2\Psi}{\partial(\varphi/2)^2} + \left(\frac{E}{E_c} + \frac{E_J}{E_c}\cos\varphi\right)\Psi = 0. \tag{2.41}$$

By substituting the wave function (2.39) into the Schrödinger equation, one gets the picture of band energy spectrum and a set of related effects well known from solid state theory, such as Bloch oscillations and Zener tunneling [24]. Each of the energy bands are periodic in q as can be seen in Figures 2.5 and 2.6. The first Brillouin zone extends over $-e \leq q \leq e$.

In Figure 2.5 the dispersion curve $E(k)$ of the Hamiltonian (2.38) has been drawn in the strong coupling regime for the three lowest energy bands. In the weak coupling regime the two lowest dispersion curves of the Hamiltonian (2.38) look something like in Figure 2.6. The energy has been approximated

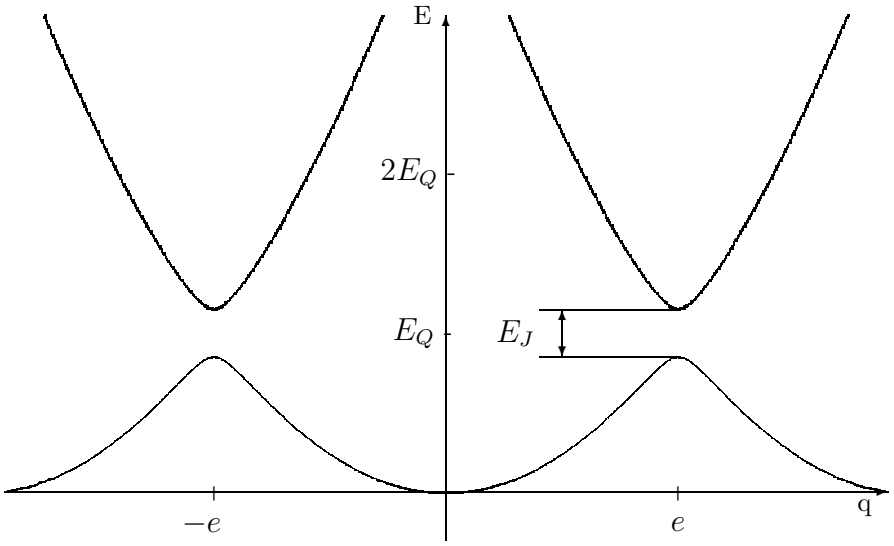

Figure 2.6: Dispersion curves of the energy bands of Hamiltonian (2.38) with with ratio $E_c/E_J = 2.5$.

by the formula [25]

$$E(q) = \frac{1}{2}\Big[q^2 + (|q| - 2)^2 \pm \sqrt{\big((|q| - 2)^2 - q^2\big)^2 + E_J}\Big] \tag{2.42}$$

The Quantum Langevin Equation For q

The analogy between a small Josephson junction and an electron in a crystal lattice fails as soon as even a weak interaction between the junction and the set of coordinates of the system of the junction quasiparticles, which plays the role of a "heat bath" (i.e. the junction environment), is taken into account. As discussed above, the junction has to be taken as a single macroscopic quantum object which alone represents the total statistical ensemble. Accordingly, if the temperature T is low enough,

$$k_B T \ll \Delta^{(0)} \tag{2.43}$$

where $\Delta^{(0)}$ is the energy gap between the lowest and the next energy band, the junction will be confined in the lowest band. Later it is also shown that the same conclusion is valid if there exists a small but nonvanishing external current $I(t)$. [22]

Throughout the discussion presented here, it has silently been assumed that the development of the system is adiabatic, i.e. the voltage V across the junction is not very large,

$$e|V| \ll \Delta_{1,2}(T) \tag{2.44}$$

where $\Delta_{1,2}$ are the energy gaps in the superconducting electrodes. In the single-band approximation this assumption leads to a Langevin-type of equation for the junction quasicharge as done in Reference [22]

$$\dot{q} = I(t) - GV - \tilde{I}(t). \tag{2.45}$$

Here G is the quasiparticle conductivity for low voltages and $\tilde{I}(t)$ describes the current fluctuations. The voltage V can be written in the single-band approximation as $dE^{(0)}/dq$.

Bloch-Wave Oscillations

Let us analyze the situation where the current fluctuations $\tilde{I}(t)$ are so small that they can be neglected. Now the quasicharge q and the voltage V can be considered as well-determined classical variables

$$q = q_0(t), \quad V = V_0(t) = (dE^{(0)}/dq)_{q=q_0} \tag{2.46}$$

By taking the time average of Eq. (2.45) one gets

$$\bar{V} = G^{-1}(\bar{I} - \bar{\dot{q}}). \tag{2.47}$$

If the dc current $\bar{I}$ exceeds the threshold value

$$I_t = G^{-1}[dE^{(0)}/dq]_{max} \tag{2.48}$$

it induces periodic oscillations of q and V with the frequency [22]

$$\omega_B = (\pi/e)(\bar{I} - G\bar{V}). \tag{2.49}$$

These are just the exact analog of the so-called Bloch oscillations, which can arise in space-periodic conducting solid under the action of an intense electric field [22]. The Bloch oscillations correspond to reflections from Brillouin zone boundaries.

The description of the Bloch-wave oscillations is translated to the Josephson junction language in Reference [22]. In short, the Bloch-wave oscillations are

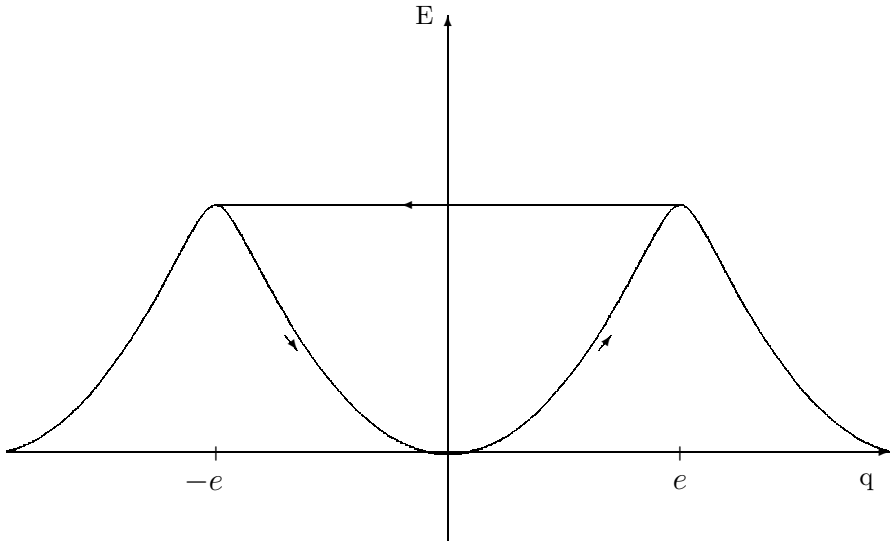

Figure 2.7: Bloch oscillation on the lowest energy band in the limit $E_J \ll E_Q$.

just the process of a periodic discrete transfer of Cooper pairs between the junction electrodes, interposed by a recharging of the junction capacitance by the external current. The basic Bloch oscillation process is sketched in Figure 2.7.

Besides the Bloch-oscillations, the usual Josephson oscillations (2.18) are always present in the junction, but the amplitude of these oscillations vanishes in the present limit. [22]

The Bloch-wave oscillations have been observed in single Josephson junctions by D. B. Haviland et al. [26]

Zener tunneling

If the external current $\bar{I}(t)$ is kept small, the junction keeps Bloch oscillating in the lowest energy band. But, if the current is increased, the Bloch oscillations are suppressed because of the transitions of the system to the higher energy bands become more probable [27]. This is an exact analog to Zener tunneling, which occurs when electrons in a periodic potential are under influence of an electric field [24]. This kind of "jumps" to higher energy bands are possible already for exponentially small Zener tunneling probabilities. When the system is transferred to a higher band it starts to oscillate only if the external current

$\bar{I}$ exceeds a threshold current similar to Equation (2.48)

$$I_t = G^{-1}[dE^{(1)}/dq]_{max}. \tag{2.50}$$

Otherwise, the state of the system becomes stationary on the higher band. However, it is possible for the system to transfer to even higher bands. This corresponds to an unlimited growth of the voltage across the junction in time. [28]

The above picture is valid only when one neglects the effects of dissipation, i.e. if one describes the junction dynamics with Hamiltonian (2.38) [28]. In real systems the junction is in connection with its environment and the dissipation gives rise to relaxation to lower bands [29]. These relaxation processes stabilize the system and lead to the existence of a crossover between the regime of Bloch oscillations in the lowest energy band and dissipative dynamics of the quasicharge in higher bands [29]. The Bloch oscillations make also possible the building of a novel type of transistor, namely the Bloch Oscillating Transistor (BOT) [30, 31].

2.2.5 Complementary Effects

K. K. Likharev and A. B. Zorin have proposed [22] that the "classical" Josephson effects and the Bloch-wave effects are conjugated in the sense that the Josephson coupling should lead to one of these effects, depending on the junction parameters. Later experimental observations [26] have confirmed their proposition. In the limit of $E_J \to 0$ the quasicharge q is nearly a classical quantity and Bloch-wave oscillations and related effects take place. In the opposite limit, where $E_c \to 0$, one has the phase difference φ as a classical variable and gets the usual Josephson effects. Both of these effects occur at $T = 0$ and $I = 0$ but become unstable with respect to small currents and thermal fluctuations which lead to quantum fluctuations of q or φ and to nonlinear effects. [22]

Chapter 3

Charge Transport in Small Tunnel Junctions

"To retain respect for sausages and laws, one must not watch them in the making."
- Otto von Bismarck

In the previous chapter it was discussed that to see the single charge effects in an ultrasmall tunnel junction, the junction properties have to satisfy two conditions. Firstly, the charging energy E_c of a single electron has to be larger than the thermal energy k_BT in order to avoid thermal fluctuations. Secondly, the tunneling resistance R_T of the junction has to be larger than the so called resistance quantum R_Q. This is to avoid the quantum fluctuations of charge. Furthermore, the junction was coupled with an ideal voltage source which results in constant charge on the junction capacitor. The tunneling current through the junction defined the tunnel resistance. In this way the current-voltage characteristic are of the same form as for an Ohmic resistor (see Figure 3.1). This kind of description of the behaviour of the tunnel junction is called the *global view*.

However, this is not the only way to describe junction dynamics. In the next section the local view of a tunnel junction is discussed. Then a description of the junction environment is presented. Finally, there is some discussion of tunneling rates in Josephson junctions and in double junction systems. This chapter is based on the review by Ingold and Nazarov [17].

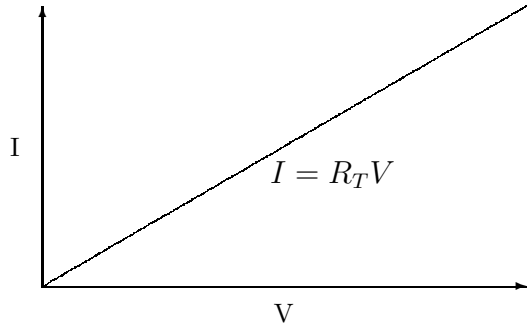

Figure 3.1: Current-voltage characteristic of the global view.

3.1 Local View of a Tunnel Junction

Instead of connecting the tunnel junction to an ideal voltage source, consider a case where an ideal external current I controls the junction charge. Again, because the current is a continuous variable, the junction can be charged continuously, even in fractions of elementary charge. The interplay between the discrete nature of the charge of the tunneling electron and the continuous nature of the junction charge Q leads to new type of charging effects. The tunneling event in zero temperature is possible only if the difference between the charging energies in the state before and after the tunneling event is positive, i.e.

$$\Delta E = E_b - E_a = \frac{Q^2}{2C} - \frac{(Q-e)^2}{2C} = \frac{e(Q-\frac{e}{2})}{C} > 0. \tag{3.1}$$

Here b stands for before and a for after. This implies, that when $Q < e/2$ the tunneling effect will not occur. This is called the *Coulomb blockade* of tunneling. Furthermore, the current through the junction should equal to zero when the potential difference V across the junction plates satisfies $-e/2C < V < e/2C$. This means that there should exists a so called *Coulomb gap* (see Figure 3.2). The Coulomb blockade of tunneling is weakened by the thermal and quantum fluctuations of the electromagnetic environment that can activate the charge transfer across the junction [32]. On the other hand, if one considers a tunnel junction made of superconducting material, one must take into account that the charge of the tunneling particle is $2e$. Due to this, one must multiply every e in above discussion by the factor 2.

According to Equation (3.1), when one starts with a junction with charge

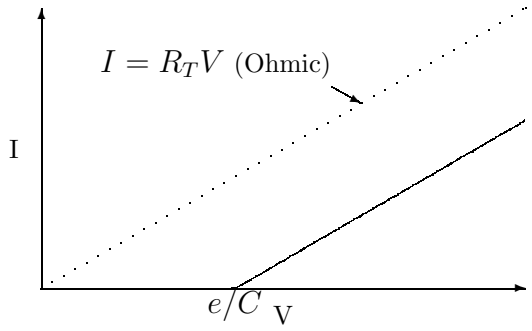

Figure 3.2: Current-voltage characteristic of the local view.

$Q < e/2$ the external current I is only charging the junction until the threshold charge $e/2$ is reached. When that happens, a tunneling event occurs and the cycle starts again. By repeating this process one gets the so called *Single Electron Tunneling* (SET) oscillations of the junction voltage V. The oscillations occur with the fundamental frequency

$$f_{SET} = I/e. \tag{3.2}$$

Similarly, with Josephson junctions, one gets the familiar Bloch oscillations (see Subsection 2.2.4) with frequency

$$f_{Bloch} = I/2e. \tag{3.3}$$

The consideration above takes into account only the energy difference (3.1), and therefore tackles solely with the junction the charge is tunneling through, ignoring its interactions with the rest of the world[1]. On the other hand, in the global view of describing the tunneling process there is no change in charging energy. The charge equilibrium is immediately restored by the voltage source, which does the work eV ($2eV$) in transfering an electron (or a Cooper pair) to charge the junction capacitor back to charge Q. So, which one of these descriptions is correct? Can the junction be taken as decoupled from its surroundings by replacing the rest of the world by ideal voltage or current source? The answer is *both* yes and no. The local and global view are correct, but only if assumptions made in them hold in the system, i.e. the junction is connected only to an ideal current or voltage source. But, if there exists some impedance

[1]Therefore the term local view.

$Z(\omega)$ in the environment, it must be taken into account. For example, the leads that connect the sources to the junction always have capacitances, that are polarized by the average voltage across the junction and therefore act as an effective voltage source [33]. Also, the electromagnetic modes of the leads and external circuit are coupled to the electric field between the plates of the junction. This affects the charge tunnling rates of the junction, as will be seen later on. All in all, tunneling in tunnel junctions cannot be modelled by describing the surroundings of the junction by ideal current and voltage sources, but instead the *impedance* of the environment must be taken into account.

3.2 Description of Environment

The Hamiltonian description of a system does not take *dissipation* into account, i.e. the energy is always conserved inside the system the Hamiltonian describes. Now, if one wants to introduce impedance $Z(\omega)$ into the system, then one is also including dissipation. How is it then possible to incorporate impedance and still stay in Hamiltonian formalism? Well, the answer is rather obvious. The Hamiltonian of the system is coupled with that of an environment. This means, that when talking about tunnel junctions the Hamiltonian of the whole junction + dissipation system consist of Hamiltonians of the junction $\mathcal{H}_J$ and the environment $\mathcal{H}_{env}$, like

$$\mathcal{H} = \mathcal{H}_J + \mathcal{H}_{env}. \tag{3.4}$$

What is the *form* of the Hamiltonian of the environment, when considering a Josephson junction? A. O. Caldeira and A. J. Leggett have introduced [34, 35] a model where the dissipation is represented by a set of harmonic oscillators that are bilinearly coupled to the phase difference φ of the junction. These harmonic oscillators can be viewed as LC-circuits and in some cases they can be justified microscopically. From now on, the tunnel junctions studied here are Josephson junctions. This way the phase difference φ is the difference between the phases of the macroscopic wave functions of the Cooper pair condensates on both sides of the junction. Now the Hamiltonian of the environment can be written as

$$\mathcal{H}_{env} = \frac{\tilde{Q}^2}{2C} + \sum_{n=1}^{N} \left[\frac{q_n^2}{2C_n} + (\frac{\hbar}{e})^2 \frac{1}{2L_n} (\tilde{\varphi} - \varphi_n)^2 \right], \tag{3.5}$$

where the first term describes the charging energy of the junction capacitor. The second term consist of the sum over the environmental degrees of freedom that are represented by harmonic oscillators with frequency $1/\sqrt{L_n C_n}$. N is the number of environmental degrees of freedom and has to be rather large. Here the $\tilde{Q}$ and $\tilde{\varphi}$ are the *fluctuations* of the charge of the junction capacitor and the phase difference of the junction plates, respectively. They are defined as

$$\begin{aligned} \tilde{Q} &= Q - CV, \\ \tilde{\varphi}(t) &= \varphi(t) - \frac{2e}{\hbar} Vt, \end{aligned} \tag{3.6}$$

where Q is the actual charge of the junction and CV is the average one imposed by the voltage source V. $\varphi(t)$ is similarly the actual (time-dependent) phase difference and $\frac{2e}{\hbar}Vt$ is the average time evolution of the phase. This change of the reference frame has been done in order to see the equivalence between the LC-circuit and a harmonic oscillator.

In the next section the rates for tunneling of Cooper pairs and quasiparticles are derived by using the description of environment presented here.

3.3 Tunneling Rates in Superconducting Junctions

3.3.1 Tunneling of Cooper Pairs

Let us first consider the case of Cooper pair tunneling in the weak coupling regime ($E_J \ll E_c$). The temperature is assumed to be very low compared to the critical temperature of the superconductor and voltages are supposed to be below the voltage $2\Delta/e$, where 2Δ is the pair binding energy. With these assumptions one can neglect quasiparticle exitations, as seen in Chapter 2. So, the tunneling events consist solely of the tunneling of Cooper pairs. The Hamiltonian is now acting in the Hilbert space of Q, φ and the environmental degrees of freedom. The Cooper pairs form a condensate and therefore do not lead to additional dynamical degrees of freedom. The total Hamiltonian (3.4) is then

$$\mathcal{H} = \mathcal{H}_{env} + E_J \cos\varphi, \tag{3.7}$$

where the environmental Hamiltonian is the one presented in Equation (3.5) and the second term gives the coupling between the superconducting regions.

One can rewrite the second term as

$$E_J \cos\varphi = \frac{E_J}{2} e^{-i\varphi} + \frac{E_J}{2} e^{i\varphi} \tag{3.8}$$

The operator $e^{-i\varphi}$ changes the charge Q on the junction by $2e$, which can be seen by calculating

$$e^{i\varphi} Q e^{-i\varphi} = e^{i\varphi} \left[Q \sum_{k=0}^{\infty} \frac{(-i)^k \varphi^k}{k!} \right] = e^{i\varphi} \left[\sum_{k=0}^{\infty} \frac{(-i)^k Q \varphi^k}{k!} \right]. \tag{3.9}$$

Now, according to the commutation relation (2.31),

$$Q\varphi = \varphi Q - 2ei \Rightarrow Q\varphi^2 = \varphi Q \varphi - 2ei\varphi = \varphi^2 Q - 4ei\varphi. \tag{3.10}$$

By induction $Q\varphi^k = \varphi^k Q - ik2e\varphi^{k-1}$. So, one gets

$$e^{i\varphi} Q e^{-i\varphi} = e^{i\varphi} \left[\sum_{k=0}^{\infty} \frac{(-i)^k (\varphi^k Q - ik2e\varphi^{k-1})}{k!} \right]. \tag{3.11}$$

This is equivalent to

$$e^{i\varphi} Q e^{-i\varphi} = e^{i\varphi} \left[\sum_{k=0}^{\infty} \frac{(-i)^k \varphi^k Q}{k!} \right] - e^{i\varphi} \left[\sum_{k=1}^{\infty} \frac{(-i)^k ik2e\varphi^{k-1}}{k!} \right], \tag{3.12}$$

from which

$$e^{i\varphi} Q e^{-i\varphi} = e^{i\varphi} e^{-i\varphi} Q - e^{i\varphi} \left[\sum_{k=1}^{\infty} \frac{(-i)^{k-1}(-i) i2e\varphi^{k-1}}{(k-1)!} \right]. \tag{3.13}$$

And, finally one gets

$$e^{i\varphi} Q e^{-i\varphi} = Q - 2e(e^{i\varphi} e^{-i\varphi}) = Q - 2e. \tag{3.14}$$

To obtain the supercurrent through the junction let us first calculate the tunneling rates.

Calculation of tunneling rates

The tunneling rate calculation is done in terms of the Fermi's Golden Rule approximation [36]. Because the Josephson energy is considered small in the

limit at hand, the coupling can be taken as a perturbation. According to the golden rule, the transition rate to the "forward" direction is given by

$$\Gamma_{i\to f} = \frac{2\pi}{\hbar}|\langle f|E_J\cos(\varphi)|i\rangle|^2\delta(E_i - E_f). \tag{3.15}$$

This is the rate for Cooper pair trasitions between the initial state $|i\rangle$ and the final state $|f\rangle$. In the absence of the quasiparticle exitations we can write the matrix element in Equation (3.15)

$$\langle f|E_J\cos(\varphi)|i\rangle = \frac{E_J}{2}\langle R'|e^{-i\varphi}|R\rangle + \frac{E_J}{2}\langle R'|e^{i\varphi}|R\rangle \tag{3.16}$$

where $|R\rangle$ and $|R'\rangle$ are charge states with energies E_R and $E_{R'}$. To calculate the total rate for Cooper pairs from "left" to "right" one has to sum over all initial states R weighted with the probability $P_\beta(R)$ to find these states and over all final states R'. So the forward tunneling rate is

$$\overrightarrow{\Gamma}(V) = \frac{2\pi}{\hbar}\left(\frac{E_J}{2}\right)^2\sum_{R,R'}|\langle R'|e^{-i\varphi}|R\rangle|^2 P_\beta(R)\delta(E_R - E_{R'}) \tag{3.17}$$

The delta function can be rewritten in terms of its Fourier transform:

$$\delta(E_R - E_{R'}) = \frac{1}{2\pi\hbar}\int_{-\infty}^{\infty} dt\exp\Big(\frac{i}{\hbar}(E_R - E_{R'})t\Big). \tag{3.18}$$

The tunneling rate can now be written as

$$\overrightarrow{\Gamma}(V) = \frac{E_J^2}{4\hbar^2}\int_{-\infty}^{\infty} dt\sum_{R,R'}\langle R|e^{\frac{i}{\hbar}\hat{\mathcal{H}}t}e^{i\varphi}e^{-\frac{i}{\hbar}\hat{\mathcal{H}}t}|R'\rangle\langle R'|e^{-i\varphi}|R\rangle P_\beta(R). \tag{3.19}$$

The time dependence can be included in the phase operator by switching to Heisenberg picture where the time dependent phase operator is defined as [37]

$$\varphi(t) = e^{\frac{i}{\hbar}\hat{\mathcal{H}}t}\varphi e^{-\frac{i}{\hbar}\hat{\mathcal{H}}t}. \tag{3.20}$$

At $t = 0$ the operators are the same in both representations [37],

$$\varphi(0) = \varphi. \tag{3.21}$$

Therefore,

$$e^{\frac{i}{\hbar}\hat{\mathcal{H}}t}e^{i\varphi}e^{-\frac{i}{\hbar}\hat{\mathcal{H}}t}\varphi = e^{i\varphi(t)}, \tag{3.22}$$

$$e^{-i\varphi} = e^{-i\varphi(0)}. \tag{3.23}$$

Now the tunneling rate is of form

$$\overrightarrow{\Gamma}(V) = \frac{E_J^2}{4\hbar^2}\int_{-\infty}^{\infty} dt \sum_{R,R'} \langle R|e^{i\varphi(t)}|R'\rangle\langle R'|e^{-i\varphi(0)}|R\rangle P_\beta(R). \tag{3.24}$$

According to Equation (3.6) $\varphi(0)$ can be written as $\varphi(0) = \tilde{\varphi}(0)$. Also, if Equation (3.24) is multiplied and divided by $e^{\frac{i}{\hbar}2eVt}$ it becomes

$$\begin{aligned}\overrightarrow{\Gamma}(V) = \frac{E_J^2}{4\hbar^2}\int_{-\infty}^{\infty} dt \exp\Big(\frac{i}{\hbar}2eVt\Big) \sum_{R,R'} \langle R|e^{i\varphi(t)-\frac{2eVt}{\hbar}}|R'\rangle \\ \times \langle R'|e^{-i\tilde{\varphi}(0)}|R\rangle P_\beta(R).\end{aligned} \tag{3.25}$$

The term $\varphi - \frac{2eVt}{\hbar}$ can also be written according to Equation (3.6), arriving thus at

$$\overrightarrow{\Gamma}(V) = \frac{E_J^2}{4\hbar^2}\int_{-\infty}^{\infty} dt \exp\Big(\frac{i}{\hbar}2eVt\Big) \sum_{R,R'} \langle R|e^{i\tilde{\varphi}(t)}|R'\rangle\langle R'|e^{-i\tilde{\varphi}(0)}|R\rangle P_\beta(R). \tag{3.26}$$

Because the charge states form a complete set, the sum over all R' is an identity operator and

$$\overrightarrow{\Gamma}(V) = \frac{E_J^2}{4\hbar^2}\int_{-\infty}^{\infty} dt \exp\Big(\frac{i}{\hbar}2eVt\Big) \sum_{R} \langle R|e^{i\tilde{\varphi}(t)}e^{-i\tilde{\varphi}(0)}|R\rangle P_\beta(R), \tag{3.27}$$

and together with definition of the equilibrium correlation function

$$\langle e^{i\tilde{\varphi}(t)}e^{-i\tilde{\varphi}(0)}\rangle = \sum_{R} \langle R|e^{i\tilde{\varphi}(t)}e^{-i\tilde{\varphi}(0)}|R\rangle P_\beta(R) \tag{3.28}$$

the tunneling rate is obtained

$$\overrightarrow{\Gamma}(V) = \frac{E_J^2}{4\hbar^2}\int_{-\infty}^{\infty} dt \exp\Big(\frac{i}{\hbar}2eVt\Big) \langle e^{i\tilde{\varphi}(t)}e^{-i\tilde{\varphi}(0)}\rangle. \text{ [17]} \tag{3.29}$$

The equilibrium correlation function (3.28) can be simplified by using the generalized Wick theorem for equilibrium correlation functions, as done in Reference [17]. By doing so, one gets

$$\langle e^{i\tilde{\varphi}(t)}e^{-i\tilde{\varphi}(0)}\rangle = e^{\langle[\tilde{\varphi}(t)-\tilde{\varphi}(0)]\tilde{\varphi}(0)\rangle}. \tag{3.30}$$

Equation (3.30) can be expressed in terms of the phase-phase correlation function

$$J(t) = \langle\big[\tilde{\varphi}(t) - \tilde{\varphi}(0)\big]\tilde{\varphi}(0)\rangle. \tag{3.31}$$

For the use in Equation (3.29) it is useful to introduce the Fourier transform of the correlation function (3.30), which is denoted by $P(E)$

$$P(E) = \frac{1}{2\pi\hbar}\int_{-\infty}^{\infty} dt \exp\Big(J(t) + \frac{i}{\hbar}Et\Big). \tag{3.32}$$

Finally, the tunneling rate for the Cooper pairs is given by

$$\overrightarrow{\Gamma}(V) = \frac{\pi E_J^2}{2\hbar}P(2eV). \tag{3.33}$$

A corresponding calculation can be done for the backward tunneling rate, but it is obvious from symmetry reasons that [17]

$$\overleftarrow{\Gamma}(V) = \overrightarrow{\Gamma}(-V). \tag{3.34}$$

The discussion presented above has considered only the weak coupling regime, where the charge is well defined and the phase fluctuates. In the limit of large Josephson coupling energy ($E_J \ll E_c$) the phase is localized in one of the wells in the "tilted-washboard" potential. The tunneling rates in this limit could be derived similarly. They can also be obtained with the phase-charge duality transformations presented in Reference [17]. This is the process dual to the tunneling of Cooper pairs in the weak coupling regime, and involves incoherent tunneling of the phase.

Supercurrent Through the Junction

From the rate expression (3.33) and the symmetry (3.34) the supercurrent is immediately obtained [17]

$$I_S(V) = 2e\big(\overrightarrow{\Gamma}(V) - \overleftarrow{\Gamma}(V)\big) = \frac{\pi e E_J^2}{\hbar}\big(P(2eV) - P(-2eV)\big). \tag{3.35}$$

Here it is taken into account that each tunneling process transports a charge of $2e$. This result is equivalent to the fact that each Cooper pair tunneling carries an energy $2eV$ in the direction of applied field. Because Cooper pairs do not have kinetic energy to absorb a part of $2eV$, this energy has to be transferred to the environment. The probability of this transfer is $P(E)$. One sees from (3.35) that the supercurrent is directly proportional to the probability $P(E)$. This makes it possible to measure the properties of the environment directly. [17]

General Properties of $P(E)$ and $J(t)$

The phase-phase correlation function (3.31) can be written in terms of the real part of the total impedance. It is done in Reference [17] using the fluctuation-dissipation theorem and it says that

$$J(t) = \frac{1}{2}\int_0^\infty \frac{d\omega}{\omega}\frac{ReZ_t(\omega)}{R_Q}\left\{ \coth\left(\frac{1}{2}\beta\hbar\omega\right)\big[\cos(\omega t) - 1\big] - i\sin(\omega t)\right\}. \quad (3.36)$$

Here the $Z_t(\omega)$ is total impedance of the system and can be written in terms of the total impedance of the junction parallel with the environmental impedance

$$Z_t(\omega) = \frac{1}{i\omega C + Z^{-1}(\omega)}. \quad (3.37)$$

The $P(E)$ can now be calculated if the total impedance is known. For example, if the total impedance is zero the $P(E)$ transforms into a delta function:

$$P(E) = \frac{1}{2\pi\hbar}\int_{-\infty}^{\infty} \exp\left(0 + \frac{i}{\hbar}Et\right) = \delta(E). \quad (3.38)$$

Analytically it is, however, impossible except for some special cases. There are nonetheless general properties which are independent of the impedance. They are proven in Reference [17] and only listed here:

$$\int_{-\infty}^{\infty} dE P(E) = 1, \quad (3.39)$$

$$\int_{-\infty}^{\infty} dE E P(E) = \frac{e^2}{2C}, \quad (3.40)$$

$$P(-E) = e^{-\beta E}P(E). \quad (3.41)$$

Here $\beta = 1/k_B T$ where k_B is the Boltzmann constant and T is the temperature. The first relation is a confirmation of the interpretation of $P(E)$ as probability. The last of the relations means that the probability to excite environmental modes compared to the probability to absorb energy from the environment is larger by a Boltzmann factor. It also says that at zero temperature there can be no energy absorption from the environment when $P(E)$ vanishes for negative energies.

3.3.2 Tunneling of Quasiparticles

In Josephson junctions also quasiparticle tunneling can exist, in addition to Cooper pair tunneling. Let us first consider the quasiparticle density of states

obtained from the BCS-theory [7]

$$\frac{N_S(E)}{N(0)} = \begin{cases} \frac{|E|}{(E^2-\Delta^2)^{1/2}} & \text{for } |E| > \Delta \\ 0 & \text{for } |E| < \Delta \end{cases} \tag{3.42}$$

where the density of states is taken relative to the density of states in the normal metal at Fermi level. 2Δ is the magnitude of the superconducting gap within which the quasiparticle density of states vanishes. With the help of this equation one is able to determine the forward tunneling rate as done in Reference [17] and arrive at

$$\begin{aligned} \overrightarrow{\Gamma}(V) =& \frac{1}{e^2 R_T} \int_{-\infty}^{\infty} dE dE' \frac{N_S(E) N_S(E'+eV)}{N(0)^2} \\ & \times f(E)\big[1 - f(E'+eV)\big] P'(E-E'). \end{aligned} \tag{3.43}$$

Here the $f(E) = 1/[1+\exp(\beta E)]$ are Fermi functions and the probability to exchange energy with the environment is given by

$$P'(E) = \frac{1}{2\pi\hbar} \int_{-\infty}^{\infty} \exp\left(J'(t) + \frac{i}{\hbar} E t\right) \tag{3.44}$$

which differs from (3.32) in terms of the phase-phase correlation function[2] that is slightly different than in (3.31) because the phase fluctuations differ due to the charge carried by quasiparticles is only e.

By using the symmetry relation (3.34), the detailed balance symmetry (3.41) and the properties of the Fermi function, it is possible to write the quasiparticle current as [17]

$$\begin{aligned} I_{qp} =& \frac{1}{eR_T} \int_{-\infty}^{\infty} dE dE' \frac{N_S(E') N_S(E'+E)}{N(0)^2} \frac{1 - e^{-\beta eV}}{1 - e^{-\beta E}} \\ & \times P'(eV - E)\big[f(E') - f(E'+E)\big] \end{aligned} \tag{3.45}$$

The quasiparticle tunneling between two superconductors can be used in measuring the superconducting energy gap as done in References [38]- [40].

3.3.3 Suppression of the Coulomb Blockade

The quantum mechanical nature of the electromagnetic environment can severly reduce the Coulomb charging effects discussed in Section 3.1. The tunneling electron has to excite electromagnetic modes of the coupled system formed

[2] This is, in fact, the same P'(E) as one would get for the normal metal tunnel junction by doing the same kind of calculations as done for the superconducting one.

by the junction and its electromagnetic environment to change the charge on the junction capacitor and thus lead to the Coulomb effect [41]. The energy of these modes is quantized so they will be excited only if the voltage V across the junction reaches $\hbar\omega/e$. An increase of the impedance of the environment strengthens the coupling of the junction to low-frequency modes. Thereby, the charging effects are usually observable when the junction is placed in a very high-impedance environment or for large voltages.

The above situation has a straight mechanical analoque in the solid state physics, namely the Mössbauer effect. In the Mössbauer effect the γ quanta (photons) that impinge upon nuclei of atoms in a lattice can excite nuclear transitions in ways that would be forbidden if the lattice were not present. The γ quanta are emitted by, for example, a radioactive nucleus that is embedded in crystal. There are two possible ways to satisfy momentum conservation when a γ quantum is emitted. The first is to excite phonons in a crystal, which means that the momentum is transferred to the emitting nucleus and the energy of the γ quantum is reduced. The second possibility is the so called Mössbauer transition in which the recoil momentum is transferred to the whole crystal. The recoilless transitions are favored if it is difficult to excite phonons. If the mass of the crystal is large the energy of the γ quantum and the momentum of the nucleus remain unchanged.

In ultrasmall tunnel junctions the emission of the γ quantum is identified as the tunneling of an electron. The momentum of the nucleus is related to the charge of the junction. If the charge is kept fixed there is no Coulomb blockade which compares to the Mössbauer transition. There is no excitation of the environmental modes. If the charge of the junction is changed the Coulomb blockade is obtained and the situation is analogous to the non-Mössbauer transition. This requires excitations of environmental modes. So the Coulomb blockade is only possible if there are low frequency environmental modes coupled strongly to the tunneling electron, which means that a high impedance environment is needed. [17]

3.4 Circuits of Tunnel Junctions

The lenghty derivations of the $P(E)$-function in the previous section could have been skipped[3] just by defining the $P(E)$ as the probability of the tunneling

[3]At least, in the context of this thesis.

electron to transfer energy to electromagnetic modes of the circuit, and by saying that this probability depends on the impedance $Z(\omega)$ of the environment of the junction. However, based on Equations (3.32) and (3.35), one is able to determine the IV-characteristics of the junction, at least in some special cases. One gets on the grounds of the $P(E)$, that the charging effects are observable only, when the environmental impedance is of the order of the resistance quantum R_Q [17]. This sets some practical limitations, since a very high resistance has to be placed near the junction in order to see the charging effects. This large resistance heats the junction and therefore prevents the desired effects to occur (see Equation (2.5)). Additionaly, the leads effectively provide a voltage bias and cause large zero-point fluctuations of the charge on the junction plates, and therefore wash out the single charge effects.

So, a single junction connected to an electromagnetic environment is not a very practical starting point, if one wants to see the effects of the single charge tunneling. Intuitively, the next wise step is to study multijunction systems and try to observe these effects in them. As an example, a Single Electron Transistor (SET) is examined in the following subsections, both in the normal and superconducting case.

3.4.1 Single Electron Transistor

The SET consists of two tunnel junctions connected in series and driven by voltage V. As a consequence, there exists a metallic island between the two junctions. This island is connected to a control voltage V_g source via a capacitor C_g. These are called as the *gate voltage* and *gate capacitance*, respectively. A circuit diagram is presented in Figure 3.3 where N describes the number of excess electrons on the island compared with the positive charge (protons) on the island. The first observations of single charge tunneling were made with this device by T. A. Fulton and G. J. Dolan [42]. Let us now analyze this circuit a little bit.

First of all, the total capacitance C of the two tunnel junctions is obtained by equating in standard way

$$\frac{1}{C} = \frac{1}{C_1} + \frac{1}{C_2} = \frac{C_1 + C_2}{C_1 C_2}, \tag{3.46}$$

which implies

$$C = \frac{C_1 C_2}{C_1 + C_2}. \tag{3.47}$$

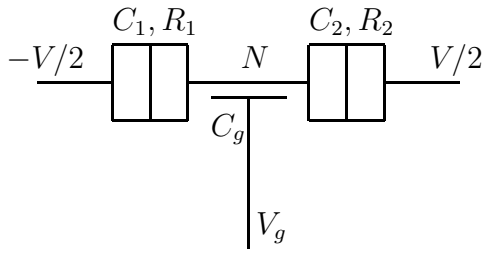

Figure 3.3: The single electron transistor.

Also, the potential difference across the whole two junction system is $U = Q_1/C_1 + Q_2/C_2$, where Q_1 and Q_2 are the charges on the junction 1 and 2, respectively (see Fig. 3.3). Therefore, one has for the total charge of the two junction system as seen from the outside

$$Q = CU = \left(\frac{C_1 C_2}{C_1 + C_2}\right)\left(\frac{Q_1}{C_1} + \frac{Q_2}{C_2}\right) = \frac{Q_1 C_2 + Q_2 C_1}{C_1 + C_2}. \tag{3.48}$$

In this way the two junctions are described as one, and therefore, based on the discussion made in Chapter 2, one can take the total charge Q as a continuos variable. On the other hand, the charge on the island can change only when an electron tunnels to or from the island. This implies that the island charge is an integer multiple of the elementary charge, i.e.

$$Q_1 - Q_2 = Ne. \tag{3.49}$$

This means that the charge on the island is *quantized*. The charging energy of the capacitors can now, according to Equations (3.48) and (3.49) be written in terms of Q_1 and Q_2 or Q and Ne

$$\frac{Q_1^2}{2C_1} + \frac{Q_2^2}{2C_2} = \frac{Q^2}{2C} + \frac{(Ne)^2}{2(C_1 + C_2)}. \tag{3.50}$$

So, one cannot describe the double junction system simply by single junction with capacitance C, because the charging energy contains a contribution arising from the island charge.

The treatment of the transistor presented above has not taken into account the effect of the gate capacitor and voltage. As can be seen in the following,

the effect of adding these leads to a (continuous) shift of the island charge by $Q_0 = C_g V_g$. The charge on the island is now

$$Ne = Q_1 - Q_2 - Q_g. \tag{3.51}$$

According to Kirchhoff's rules, one gets two equations for voltages

$$\frac{V}{2} - \frac{Q_1}{C_1} - \frac{Q_g}{C_g} + V_g = 0 \tag{3.52}$$

$$-\frac{V}{2} + \frac{Q_1}{C_1} - \frac{Q_g}{C_g} + V_g = 0. \tag{3.53}$$

So, one has three equations for three unknown variables, i.e. Q_1, Q_2 and Q_g. By solving the group of three linear equations (3.51)-(3.53) one ends up with

$$Q_1 = \frac{C_1}{C_\Sigma}\left[\left(C_2 + \frac{C_g}{2}\right)V + C_g V_g + Ne\right] \tag{3.54}$$

$$Q_2 = -\frac{C_2}{C_\Sigma}\left[-\left(C_1 + \frac{C_g}{2}\right)V + C_g V_g + Ne\right] \tag{3.55}$$

$$Q_g = -\frac{C_g}{C_\Sigma}\left[\frac{1}{2}(C_2 - C_1)V - (C_1 + C_2)V_g + Ne\right], \tag{3.56}$$

where $C_\Sigma = C_1 + C_2 + C_g$. These equations describe the electrostatic equilibrium of the transistor.

If it is now assumed that an electron has tunneled through the left junction onto the island, then the island charge has changed from Ne to $(N-1)e$. Accordingly, the charge on the plates of the junction 1 has changed from Q_1 to $Q_1 - e$. If one replaces N with $(N-1)$ in the equilibrium equations (3.55)-(3.56), one will not result in charge $Q_1 - e$. Therefore, the new charges $Q_1 - e$, Q_2 and Q_g do not describe an equilibrium state. Instead, the changes in the charges before and after the tunneling processes are due to the work done by the voltage sources and, according to the equations (3.55)-(3.56), are of form

$$\delta Q_1 = -\frac{C_1}{C_\Sigma}e \tag{3.57}$$

$$\delta Q_2 = \frac{C_2}{C_\Sigma}e \tag{3.58}$$

$$\delta Q_g = \frac{C_g}{C_\Sigma}e. \tag{3.59}$$

Disregarding the energy transfer to and from the environmental modes, the energy that determines the tunneling rates is the difference in the electrostatic

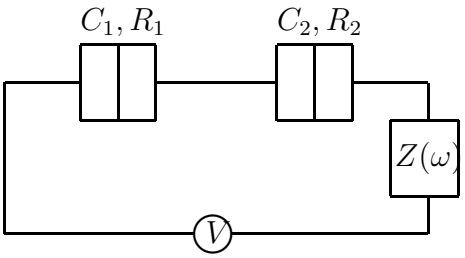

Figure 3.4: Double junction system coupled to a voltage source V via impedance $Z(\omega)$.

energy of the entire circuit. This energy difference now consists of conributions of the work done by the voltage sources V and V_g which do not change in the tunneling process. Additionally to a single junction case there exists also a contribution $(Ne)^2/2C_\Sigma$ that depends on the island charge. Therefore, the difference in the electrostatic energy before and after a tunneling event through the first junction on the left onto the island is

$$\begin{aligned}\Delta E &= \frac{(Ne)^2}{2C_\Sigma} - \frac{\big[(N-1)e\big]^2}{2C_\Sigma} - \frac{V}{2}(\delta Q_1 + e) + \frac{V}{2}\delta Q_2 + V_g \delta Q_g \\ &= \frac{e}{C_\Sigma}\left[\left(C_2 + \frac{C_g}{2}\right)V + C_g V_g + Ne - \frac{e}{2}\right].\end{aligned} \tag{3.60}$$

One has to add an extra elementary charge to δQ_1 because the charge transferred by the voltage source is diminished by $-e$ due to the electron tunneling through the left junction. From this it can be seen that the work done by the gate voltage leads to an effective island charge $q = Ne + C_g V_g$. The fact that the gate voltage V_g is a continuous variable leads to a continuous $Q_0 = V_g C_g$. This is of great importance when the SET is used as an electrometer, as will be seen later.

Tunneling Rates in SET

The tunneling rates of the SET could be calculated as in a single junction case by using second order perturbation theory (Fermi's Golden Rule). But instead, they are done here by exploiting the properties of the rates of a single tunnel junction. The double junction system studied here is the Figure 3.4. In this system C_g is assumed to be small compared to the junction capacitances C_i

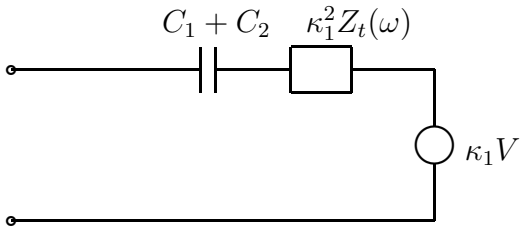

Figure 3.5: An equivalent effective circuit for tunneling through the first junction.

$(i = 1, 2)$. Therefore, it can be neglected when considering the capacitance of the system. However, the gate voltage V_g is assumed to be sufficiently large to cause the offset $V_g C_g$. By using Norton and Thevenin configurations one is able to transform the double junction circuit (Figure 3.4) to an equivalent effective circuit for tunneling through the first junction, as done in Reference [17]. This effective circuit is presented in Figure 3.5. One could do similar transform to the other junction and end up with identical circuit where only κ_1 has transformed to κ_2. The two kappa's are defined as

$$\kappa_i = \frac{C}{C_i} \quad (i = 1, 2), \tag{3.61}$$

and are a straight consequence of the Thevenin-Norton treatment. The C is the total capacitance of the circuit defined in Equation (3.47). Because C is always smaller than the smallest of the capacitances C_i, the κ_i's are therefore always less than one. Accordingly,

$$\kappa_1 + \kappa_2 = \frac{C}{C_1} + \frac{C}{C_2} = \frac{C_2 + C_1}{C_1 C_2} C = 1. \tag{3.62}$$

Also, the total impedance $Z_t(\omega)$ is of the form

$$Z_t(\omega) = \frac{1}{i\omega C + Z^{-1}(\omega)}, \tag{3.63}$$

where C is defined again as in Equation (3.47) and $Z(\omega)$ is the environmental impedance.

According to the Figure 3.5, the two junction system behaves in the tunneling processes just like a *single* junction, with appropriate tunneling capacitance C, reduced voltage $\kappa_i V$ and reduced environmental impedance $\kappa_i^2 Z_t(\omega)$.

Therefore, one is able to write the probabilities of the electron to transfer energy E with the environment, when tunneling through the i^{th} junction, like in Equation (3.44)

$$P'(\kappa_i, E) = \frac{1}{2\pi\hbar}\int_{-\infty}^{\infty} \exp\Big(\kappa_i^2 J'(t) + \frac{i}{\hbar}Et\Big). \tag{3.64}$$

The $J'(t)$ is phase-phase correlation function for the normal metal junction. The energy difference between before and after an electron tunnel process through i^{th} junction is due to the work done by reduced voltage source and difference between the charging energies of the island charge

$$\begin{aligned}\Delta E_i &= \kappa_i eV + \frac{q^2}{2(C_1+C_2)} - \frac{(q-e)^2}{2(C_1+C_2)} \\ &= \kappa_i eV + \frac{e(q-e/2)}{C_1+C_2} \quad (i=1,2),\end{aligned} \tag{3.65}$$

where $q = Ne + V_g C_g$ is the effective island charge. Now, one is able to write the forward tunneling rate through the first junction as

$$\overrightarrow{\Gamma}_1(V,q) = \frac{1}{e^2 R_1}\int_{-\infty}^{+\infty} dE \frac{E}{1-\exp(-\beta E)} P'(\kappa_1, \Delta E_1 - E), \tag{3.66}$$

where R_1 is the tunneling resistance of the first junction. Actually, the rate formula has been previously derived only for the superconducting junction, but the one for normal junction is somewhat similar and can be read from Reference [17]. Now, if the environmental impedance is low, the $P'(\kappa_1, E) \approx \delta(E)$ (according to Equation (3.38)) and the tunneling rate through the first junction can be written as

$$\overrightarrow{\Gamma}_1(V,q) = \frac{1}{e^2 R_1}\frac{\Delta E_1}{1-\exp(-\beta\Delta E_1)}. \tag{3.67}$$

For zero temperatures $1/(1-\exp(-\beta x)) = \Theta(x)$, where $\Theta(x)$ is a unit step function. This way one gets

$$\overrightarrow{\Gamma}_1(V,q) = \frac{1}{e^2 R_1}\Delta E_1 \Theta(\Delta E_1). \tag{3.68}$$

So, at low temperatures and in low impedance environment the tunneling rate is nonzero only if $\Delta E_1 > 0$. Together with Equation (3.65) one gets for

tunneling through the first juntion onto the island

$$\begin{aligned}\kappa_1 eV + \frac{e(q-e/2)}{C_1+C_2} &= \frac{C}{C_1}eV + \frac{e(q-e/2)}{C_1+C_2} \\ &= \frac{C_2}{C_1+C_2}eV + \frac{e(q-e/2)}{C_1+C_2} > 0,\end{aligned} \tag{3.69}$$

which implies

$$V + \frac{1}{C_2}(q-e/2) > 0. \tag{3.70}$$

Because the tunneling rate (3.68) obeys also the detailed balance symmetry, as does the single junction rate, one is able to write at zero temperature

$$\overleftarrow{\Gamma}_1(V, q-e) = -\frac{1}{e^2 R_1}\Delta E_1 \Theta(-\Delta E_1). \tag{3.71}$$

One is able to do the same kind of calculations for the tunneling through the second junction and obtain the same kind of results, just changing the 1's to 2's and q to $-q$. Together with Equation (3.65) one gets four conditions under which the rates are nonvanishing

$$\overrightarrow{\Gamma_1}(V,q): \quad V + \frac{1}{C_2}(q-e/2) > 0 \tag{3.72}$$

$$\overleftarrow{\Gamma_1}(V,q): \quad V + \frac{1}{C_2}(q+e/2) < 0 \tag{3.73}$$

$$\overrightarrow{\Gamma_2}(V,q): \quad V - \frac{1}{C_1}(q+e/2) > 0 \tag{3.74}$$

$$\overleftarrow{\Gamma_2}(V,q): \quad V - \frac{1}{C_1}(q-e/2) < 0. \tag{3.75}$$

From these equations one sees immediately that if the voltage satisfies $V < \min(e/2C_1, e/2C_2) = V_{cg}$, a Coulomb blockade of tunneling exists even in the low impedance environment. This is very different from what was seen in the single junction case in the previous section. The difference arises of the charging energy of the island charge.

The voltage V_{cg} is constant if no offset charge is applied at the island. Now, if one places a charge near the island as in the SET setup, the V_{cg} becomes strongly dependent of it (see Reference [17]). In the high impedance environment one naturally also sees the Coulomb effects, with the exception that the gap voltages are higher, and therefore the effects are more easily observed.

From the tunneling rates above one is able to calculate the current through the SET as a function of the offset charge Q_0 and the transport voltage V. These voltages have been restricted below the gap voltage because analytical expressions cannot be given at the other limit. Furthermore, the situation is restricted to zero temperature and the assumptions of the low impedance environment are satisfied. The calculation for the transistor current I has been done in Reference [17] and says that

$$I(Q_0,V) = \frac{1}{2}\frac{\left(\frac{Q_0-e/2}{2C}\right)^2 - V^2}{(R_1-R_2)\frac{Q_0-e/2}{2C} - (R_1+R_2)V} \times \Theta(Q_0 - e/2 + 2CV)\Theta(-Q_0 + e/2 + 2CV). \tag{3.76}$$

From this connection one can see that the current I through the junction can be very sensitive to changes in the offset charge Q_0. This sensitivity is essential when one is using the two junction system as a transistor or an electrometer [17].

In this subsection the so-called *second order effects*, have not been treated. They rise, for example, from the *simultaneous* tunneling of two electrons; one through the first junction onto the the island and one through the second junction from the island. This way there is a possibility to a current through the two junction system to exist, even if the system is in a Coulomb blockade state. This process is called *co-tunneling*.

3.4.2 Superconducting SET

In the previous subsection the two junctions were made of normal metal. If the material used in fabricating the junctions is, instead, superconducting, the situation is somewhat more difficult. In addition to the Cooper pair current in the superconducting junctions, there also exists a current that consists of quasiparticles. Moreover, the fluctuations in the electromagnetic environment cause also some structure to these currents. These three properties have been studied, for example, by A. Maassen van den Brink et al. [43]. But, before the current characteristics of the two superconducting junction system are discussed, let us first study the concept of the *parity* of the island charge. All the discussion in this subsection is based on Reference [3].

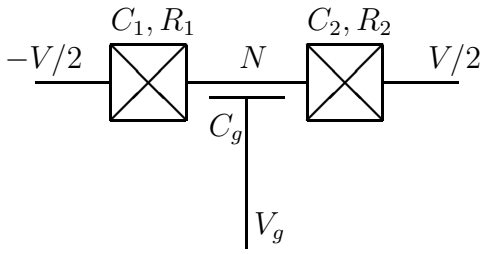

Figure 3.6: The superconducting single electron transistor.

Parity of the Superconducting Island

According to Chapter 2, in the ground state of a superconducting island all the electrons are bound as Cooper pairs. This implies that if the number N of electrons of the island is an even integer the corresponding energy of the ground state E_0 is smaller than if N is odd. Namely, an odd N means that one of the electrons in the island (that is in the ground state) does not belong to the Cooper pair condensate, i.e. it does not have a pair. Therefore it has to be a quasiparticle which has an energy that is larger than the energy of the Cooper pairs by the amount of the superconducting gap Δ. D. Averin and Yu. Nazarov have described this difference with an additive energy term, that has a value Δ when N is odd and zero when N is even [44]. At low temperatures this leads to $2e$-periodicity Q_0 depedence of the $I-V$ characteristics of the superconducting transistor. This changes to the normal metal e-periodicity when the temperature rises. These effects were observed by M. Tuominen et al. [45].

When N is even and the voltage is below $2\Delta/e$, no excitations can be created and only elastic tunneling is allowed. Also, if $E_c = e^2/2C_\Sigma \ll \Delta$ the tunneling of single electrons (i.e. quasiparticles) is omitted. In fact, if Δ is larger than all the energies that describe the system, i.e. E_J and E_c, the situation can be restricted to states where only even number of electrons lie on the island in the form of Cooper pairs. This way one can write the net charge Q of the island as $2eN$. Let us now consider a situation where the voltage bias is zero.

Superconducting Island with Zero Bias Voltage

The Hamiltonian of the two Josephson junction system with zero voltage bias can be written as

$$H = -E_1 \cos\varphi_1 - E_2 \cos\varphi_2 + \frac{(Q - Q_0)^2}{2C_\Sigma}. \tag{3.77}$$

Here E_1, φ_1 and E_2, φ_2 are the Josephson energies and phase differences of the first and second Josephson junction, respectively. $Q - Q_0$ is the island charge polarized by the gate voltage. The C_Σ is the sum of single junction capacitances and the gate junction capacitance. To make the Hamiltonian somewhat more convenient, a change of variables is made from φ_1 and φ_2 to

$$\begin{aligned} \theta &= \varphi_1 + \varphi_2 \\ \varphi &= (\varphi_2 - \varphi_1)/2. \end{aligned} \tag{3.78}$$

Here the θ is total phase difference over the whole two junction system. φ is the phase of the "internal" island and can show quantum mechanical properties. In fact, φ and the net charge Q of the island are conjugated quantum variables and obey the commutation relation (2.31). Let us now try to eliminate φ_1 and φ_2 in favor of θ and φ. With the help of trigonometry, Equation (3.77) transforms into

$$H = -E_J(\theta)\cos(\varphi - \chi) + \frac{(Q - Q_0)^2}{2C_\Sigma}, \tag{3.79}$$

where

$$\begin{aligned} E_J(\theta) &= (E_1^2 + E_2^2 + 2E_1E_2\cos\theta)^{1/2} \\ \chi &= \tan^{-1}\left[\frac{(E_1 - E_2)}{(E_1 + E_2)}\tan\frac{\theta}{2}\right]. \end{aligned} \tag{3.80}$$

Now, χ can be suppressed, because the eigenvalues of Equation (3.79) do not depend on it. So, one can rewrite

$$H = -E_J(\theta)\cos\varphi + \frac{(Q - Q_0)^2}{2C_\Sigma}. \tag{3.81}$$

If there is no polarization charge Q_0, Equation (3.81) reduces to the familiar single junction Hamiltonian. Because the Josephson energy $E_J(\theta)$ is dependent on the phase difference, the supercurrent-energy relation derived in Equation (2.2.1) must be generalized to

$$I = \frac{2e}{\hbar}\frac{\partial E}{\partial \theta}. \tag{3.82}$$

If the island capacitance C_Σ is so large that the charging energy term is effectively zero, the total energy of the system is $E = -E_J(\theta)$. This implies that the system operates in the strong coupling regime ($E_J \gg E_c$) and that the critical current of the two junction system is

$$I = -\frac{2e}{\hbar}\frac{\partial E_J(\theta)}{\partial \theta} = -\frac{2e}{\hbar}\left[\frac{1}{2E_J}(-2E_1E_2\sin\theta)\right] = \frac{2e}{\hbar}\frac{E_1E_2\sin\theta}{E_J}. \tag{3.83}$$

If the two junctions are symmetric with respect to their Josephson energies, i.e. $E_1 = E_2 = E$, the situation is reduced to

$$\begin{aligned} I &= \frac{2e}{\hbar}\frac{E^2}{E_J}\sin\theta = \frac{2e}{\hbar}\frac{E^2}{(2E^2+2E^2\cos\theta)^{1/2}}\sin\theta \\ &= \frac{2e}{\hbar}E\frac{\sin\theta}{\left[2(1+\cos\theta)\right]^{1/2}}. \end{aligned} \tag{3.84}$$

Equation (3.84) is equivalent to a current through a single junction with Josephson energy E and phase difference $\theta/2$, but only in the range $\theta \in [-\pi, \pi]$, i.e.

$$I = \frac{2e}{\hbar}E\sin\frac{\theta}{2}\ ,\ \theta \in [-\pi, \pi]. \tag{3.85}$$

The whole current I as a function of θ is shown in Figure 3.7.

On the other hand, if the two junctions are very asymmetric ($E_1 \gg E_2$) it follows that $E_J \approx E_1$ and $I = (2e/\hbar)E_2\sin\theta$. So, the current is determined entirely by the second junction.

If one considers the Hamiltonian (3.81) in the limit $E_c \gg E_J$ it is useful to express the Josephson coupling energy in the basis that consists of the eigenstates of the Cooper pair number operator N. Because $\cos\varphi = e^{i\varphi} + e^{-i\varphi}$, then according to the Equation (3.14), the Hamiltonian of the system is

$$\begin{aligned} H &= -E_J\sum_N \frac{|N+1\rangle\langle N| + |N-1\rangle\langle N|}{2} + \frac{(2eN-Q_0)^2}{2C_\Sigma} \\ &= -E_J\sum_N \frac{|N+1\rangle\langle N| + |N-1\rangle\langle N|}{2} + \frac{e^2}{2C_\Sigma}(2N-\frac{Q_0}{e})^2 \\ &= -E_J\sum_N \frac{|N+1\rangle\langle N| + |N-1\rangle\langle N|}{2} + E_c(2N-\frac{Q_0}{e})^2. \end{aligned} \tag{3.86}$$

The diagonal matrix elements of the Hamiltonian are then

$$H_{NN} = E_c\left(2N - \frac{Q_0}{e}\right)^2, \tag{3.87}$$

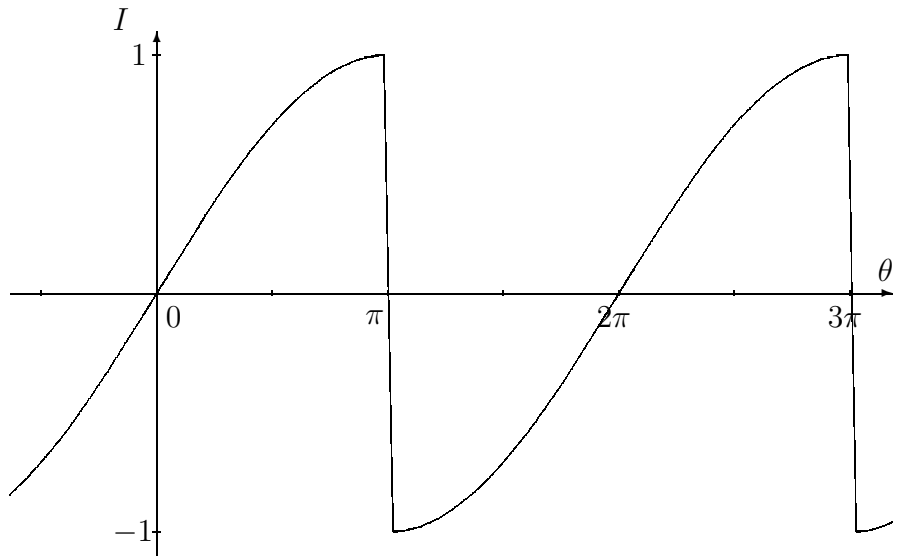

Figure 3.7: Supercurrent I through the superconducting island in the strong coupling regime. The I is measured in the units of $\frac{2eE}{\hbar}$.

and the off-diagonal elements are

$$H_{N,N\pm1} = -\frac{E_J}{2}. \tag{3.88}$$

Now one needs to find the eigenvalues of the Hamiltonian, i.e. one has to solve the Schrödinger equation

$$H\Psi = E\Psi. \tag{3.89}$$

Because the charging energy of the system is $2e$-periodic with respect the gate charge Q_0 and that the E_c and E_J are small compared with the other relevant energies of the system, the Schrödinger equation can be solved exactly. This is by solving it for two neighbouring state (N and $N+1$, e.g.) and then expanding the solution periodically. In this way the matrix representation for the Hamiltonian is

$$H_m = \begin{pmatrix} E_c(2N - \frac{Q_0}{e})^2 & -E_J/2 \\ -E_J/2 & E_c(2N + 2 - \frac{Q_0}{e})^2 \end{pmatrix}. \tag{3.90}$$

The eigenvalues of this matrix are obtained from the determinant equation

$$\begin{aligned}
&\begin{vmatrix} E_c\big(2N - \frac{Q_0}{e}\big)^2 - E & -E_J/2 \\ -E_J/2 & E_c\big(2N + 2 - \frac{Q_0}{e}\big)^2 - E \end{vmatrix} \\
&= \left[E_c\Big(2N - \frac{Q_0}{e}\Big)^2 - E\right]\left[E_c\Big(2N + 2 - \frac{Q_0}{e}\Big)^2 - E\right] - (E_J/2)^2 \\
&= 0.
\end{aligned} \tag{3.91}$$

This is of second order in E and gives straightforwardly

$$\begin{aligned}
E = E_c\Bigg[&\frac{(2N - Q_0/e)^2 + (2N + 2 - Q_0/e)^2}{2} \\
&\pm 2\left((2N + 1 - Q_0/e)^2 + (\frac{E_J}{4E_c})^2\right)^{1/2}\Bigg].
\end{aligned} \tag{3.92}$$

Using this and Equation (3.82) one obtains for the supercurrent

$$I = \frac{2e}{\hbar}\frac{E_1 E_2}{8E_c}\frac{\sin\theta}{[(2N + 1 - Q_0/e)^2 + (E_J/4E_c)^2]^{1/2}}. \tag{3.93}$$

This equation means that in the limit at hand the supercurrent depends continuously of the gate charge Q_0. This is the porperty that enables a very sensitive charge measurement with the superconducting SET (SSET). For example, when $2N + 1 = Q_0/e$ the limiting maximum value occurs

$$I = \frac{2e}{\hbar}\frac{E_1 E_2}{2E_J}\sin\theta, \tag{3.94}$$

which reduces in symmetrical case ($E_1 = E_2 = E$) to

$$I = \frac{2e}{\hbar}\frac{E}{2}\frac{\sin\theta}{\big[2(1 + \cos\theta)\big]^{1/2}}. \tag{3.95}$$

This is exactly half of the classical value in Equation (3.84).

As discussed previously, this picture is valid only when the temperature is approximately zero and biasing voltage is far below the gap voltage. However, it gives a valuable insight to the gate charge dependent current properties of the SSET. Namely, the sensitivity of the current through the SSET with respect to changes in gate charge is of great importance when one wants to measure charge precisely. The exact measurement of charge is vital, for example, if one wants to build a quantum computer using Josephson junctions. In the next subsection a brief introduction to quantum computers is given to get some motivation to study the SSETs.

3.4.3 SETs and Quantum Computers

Quantum mechanics allows the building of new kind kind of computers, namely *quantum computers*. Contrary to the ordinary computers, where the fundamental unit of information (the *bit*) is binary (i.e. its logical state is either 0 or 1), the quantum bit, *qubit*, can have a value that is 0, 1 or *both*. But how is it possible that a qubit can be in a logical state that is simultaneously both 0 and 1? Well, the answer lies in the quantum nature of the qubit. Classically speaking, at every moment a physical system is in *some* state that is determined by the system parameters, and is inherent to the system. But, contrary to the classical mechanics, in quantum mechanics the system can be in all of its so called *eigenstates* at the same time! All eigenstates appear with certain probabilities, which is called the *superposition* of the states.

A quantum computer is a device that stores information into quantum variables and processes this information conserving the quantum coherence. The quantum variable is typically any kind of physical system whose motion is effectively restricted to a two-dimensional Hilbert space [46]. These systems are quantized two-level systems and they are called *qubits* (more on quantized two-level systems in Reference [47], e.g.). Essentially any two-level system is suitable for quantum computing, as long as it fulfils the following requirements

1. The system can be prepared in the ground state.

2. The system can be controlled.

3. The system can be measured.

4. The system can be connected to its neighbours.

5. The system can be isolated from its surroundings.

These basic requirements of the quantum computing have previously been realized with the help of nuclear spins and ion traps [11].

If one couples many of these qubits together, it is imperative for the functioning of the quantum computer that the states of the qubits become *entangled*. This means that the many-particle state is no longer a product of single-particle states. Then a measurement, that is focused apparently to a single qubit, affects to the state of the whole system. A measurement of the final state of the qubit is vital for the quantum computing and the system

presented later in this thesis has a property to measure these "read-outs" as a possible application.

In Section 2.2 it was discussed that the parameters of a Josephson junction determine two of its three energy scales. It was also argued that if either one of these energies (E_J or E_c) was much larger than the other then the corresponding quantum variable (the gauge-invariant phase difference φ or the quasicharge q, respectively) would be well-defined and fluctuate only little. These regimes ($E_J \gg E_c$ and $E_c \gg E_J$) were called the strong coupling regime and the weak coupling regime. Based on this, one can build qubits whose parameters are such that the system acts on either of these two extreme regimes. When the qubit is in strong coupling regime, i.e. $E_J \gg E_c$, it is called a *phase* qubit, and when it is in weak coupling regime it is called a *charge* qubit.

As discussed above, to be able to do the read-out of the final state of the qubit is vital for doing quantum computation with the quantum computer. Previously, these read-outs for a charge qubit have been proposed to be done by radio frequency SETs (RF-SET). The problem is, however, that RF-SETs are not truly quantum-limited detectors and they have a relatively high power disspation that is required for operation, due to the fact that they consist of normal state metal. This disspation leads to heating up the surrounding qubits. In the following an alternative option is presented. It is claimed that the system described in the next chapter of this thesis is non-dissipative, does a sensitive charge detection and is quantum limited in principle.

This introduction to quantum computers has been as brief as possible and its sole purpose has been to give a meaning to measure the system presented in the following chapters. To get further information in quantum computing, Reference [48] is a good book to start with.

Chapter 4

Inductive Superconducting SET

"If you can't get rid of the skeleton in your closet, you'd best teach it to dance."
- George Bernard Shaw

If one wishes to build a quantum computer it is of great importance that one is able to do the read-out of the qubits. It has been suggested that the read out of Josephson junction qubits is made by RF-SETs. Even though the RF-SET has proven to be suitable at high-frequency charge measurements, it is imperative, due to its dissipative nature, that alternative technologies are searched. The charge detector studied in this thesis is the same one that has been measured by M. Sillanpää and co-workers at Low Temperature Laboratory in Helsinki, Finland [49, 50]. In the following section the circuit of the detector is presented. The classical and quantum mechanical models of the circuit are also presented in the subsequent sections. So, at first the general theoretical treatment of the circuit at hand is presented and thereafter, in the next chapter, the theory is used in simulations of the system.

4.1 Classical Model of the Circuit

The circuit of the inductive SSET consists of harmonic (LC) oscillator connected parallel to a SSET. It is a modification of the quantum limited electrometer presented by A. B. Zorin [51, 52]. A drawing of the circuit is shown in Figure 4.1. The system consists of two Josephson junctions which have identical tunneling resistances and Josephson energies, R_T and E_J, respectively.

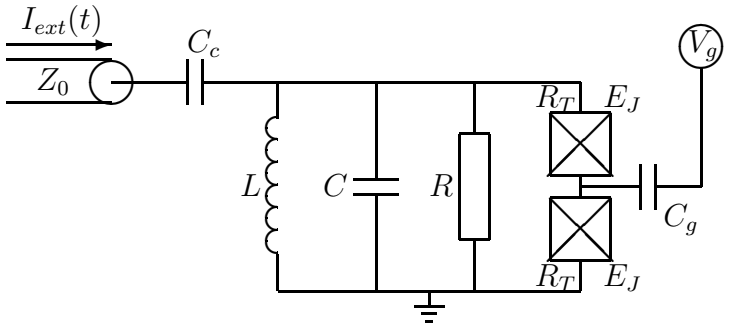

Figure 4.1: Schematic of the inductive SSET circuit.

The island between these two junctions is coupled in the usual manner to a gate voltage V_g via gate capacitance C_g. The effect of this connection is, as was seen in previous chapter, to affect the island charge and thereby the current through the two junction system. The energy gap Δ of the junctions is assumed to be so large ($\Delta \gg E_c$) that the quasiparticle tunneling effects can be neglected. The LC-circuit consists of capacitance C and inductance L and is characterized by the *natural resonance frequency* $\omega_0 = 1/\sqrt{LC}$. The effects of dissipation are modelled by the resistance R parallel to the SSET. The whole system is connected to a microwave feedline with impedance Z_0 via coupling capacitor C_c which reduces the noise reaching the sample.

Let us ignore the effects of the feedline and the coupling capacitor for a while and consider only the L-SET circuit. If one feeds external current $I_{ext}(t)$ to the circuit, one gets a current flow through each element of the circuit. The external current can be written according to Kirchhoff's rules as

$$I_{ext}(t) = I_{cond} + I_{res} + I_{ind} + I_{SSET}. \tag{4.1}$$

Here I_{cond} is the displacement current through the capacitor C and I_{res} is current through the resistor R, whereas I_{ind} and I_{SSET} stand for the currents through the inductor and the SSET, respectively. Now, basing on the previous chapter, the current through the junction pair is approximated by Equation (3.84)

$$I_{SSET} = \frac{2e}{\hbar} E_J(V_g) \frac{\sin\varphi}{\left[2(1+\cos\varphi)\right]^{1/2}},$$

where $E_J(V_g)$ is the gate tunable Josephson energy. With the help of this and common knowledge of the electrical circuitry, one can write the external

current as

$$I_{ext}(t) = C\frac{dV}{dt} + \frac{V}{R} + \frac{\int V\,dt}{L} + \frac{2e}{\hbar}E_J(V_g)\frac{\sin\varphi}{\sqrt{2(1+\cos\varphi)}}. \tag{4.2}$$

If one uses the AC Josephson relation (2.18), one gets that

$$I_{ext}(t) = C\frac{\hbar}{2e}\ddot{\varphi} + \frac{\hbar}{2eR}\dot{\varphi} + \frac{\hbar}{2eL}\varphi + \frac{2e}{\hbar}E_J(V_g)\frac{\sin\varphi}{\sqrt{2(1+\cos\varphi)}}, \tag{4.3}$$

which is the classical equation of motion of the system. It can be written in dimensionless form by dividing with $2eE_J(V_g)/\hbar$ and introducing a dimensionless time variable $\tau = \omega_p t$, with $\omega_p = \sqrt{2eI_c/\hbar C}$ and $I_c = 2eE_J(V_g)/\hbar$

$$\frac{I_{ext}(t)}{I_c} = \frac{d^2\varphi}{d\tau^2} + \frac{\hbar\omega_p}{2eRI_c}\frac{d\varphi}{d\tau} + \frac{\hbar}{2eLI_c}\varphi + \frac{\sin\varphi}{\sqrt{2(1+\cos\varphi)}}. \tag{4.4}$$

In the following, the derivative of the phase difference φ with respect to dimensionless time variable τ is for simplicity also denoted by $\dot{\varphi}$. Similarly, $d^2\varphi/d\tau^2 \equiv \ddot{\varphi}$. If the fluctuations of the phase φ are big, the sine term is negligible compared with the linear term and so the equation of motion is of form

$$\ddot{\varphi} + \frac{\hbar\omega_p}{2eRI_c}\dot{\varphi} + \frac{\hbar}{2eLI_c}\varphi - \frac{I_{ext}(t)}{I_c} = 0. \tag{4.5}$$

Because the frequency is measured in the units ω_p the factor in front of φ can be identified as the square of the resonance frequency

$$\omega_0 = \frac{1}{\sqrt{LC}}. \tag{4.6}$$

This is actually the natural resonance frequency of a simple LC-circuit.

On the other hand, when the fluctuations of the phase difference φ are small, one is able to write the sine term as $\sin\varphi \approx \varphi$ and the cosine term as $\cos\varphi \approx 1$. This way the equation of motion reduces to

$$\ddot{\varphi} + \frac{\hbar\omega_p}{2eRI_c}\dot{\varphi} + \frac{\hbar}{2eLI_c}\varphi + \frac{\varphi}{2} - \frac{I_{ext}(t)}{I_c} = 0, \tag{4.7}$$

which implies that

$$\ddot{\varphi} + \frac{\hbar\omega_p}{2eRI_c}\dot{\varphi} + \left[\frac{\hbar}{2eLI_c} + \frac{1}{2}\right]\varphi - \frac{I_{ext}(t)}{I_c} = 0. \tag{4.8}$$

Here the square root of the factor of φ times ω_p can be identified as the resonance frequency ω_r of the system

$$\omega_r = \omega_p \sqrt{\frac{\hbar}{2eLI_c} + \frac{1}{2}} = \sqrt{\omega_0^2 + \frac{\omega_p^2}{2}}. \tag{4.9}$$

So, when the fluctuations of the phase φ are increased, one can expect a shift in resonance frequency from $\omega_r \to \omega_0$. This is in fact seen in the simulations presented in the following chapter.

4.1.1 Lagrangian of the system

The equation of motion (4.3) gives the time development, i.e. the dynamics, of the system. It can be rewritten in a form

$$\begin{aligned} I_{ext}(t) = {} & C\frac{\hbar}{2e}\ddot{\varphi} + \frac{\hbar}{2eR}\dot{\varphi} \\ & - \frac{d}{d(\hbar\varphi/2e)}\left(E_J(V_g)\sqrt{2(1+\cos\varphi)} - \frac{\hbar^2}{8e^2L}\varphi^2 \right), \end{aligned} \tag{4.10}$$

similar to what was done in Subsection 2.2.1. The term

$$\frac{\hbar^2}{8e^2L}\varphi^2 - E_J(V_g)\sqrt{2(1+\cos\varphi)} \tag{4.11}$$

can be interpreted as the potential energy $\mathcal{V}$ of the system. That is,

$$\mathcal{V} = \frac{\hbar^2}{8e^2L}\varphi^2 - E_J(V_g)\sqrt{2(1+\cos\varphi)}. \tag{4.12}$$

Similarly, the term $C\hbar\ddot{\varphi}/2e$ can be written as

$$C\frac{\hbar}{2e}\ddot{\varphi} = \frac{d}{dt}\left[\frac{d}{d(\hbar\dot{\varphi}/2e)}\left(\frac{C\hbar^2}{2(2e)^2}\dot{\varphi}^2 \right) \right] = \frac{d}{dt}\left[\frac{d}{d(\hbar\dot{\varphi}/2e)}\left(\frac{CV^2}{2} \right) \right], \tag{4.13}$$

which implies that the kinetic energy $\mathcal{K}$ of the system is

$$\mathcal{K} = \frac{Q^2}{2C}. \tag{4.14}$$

Now the Lagrangian of the system is

$$\mathcal{L} = \mathcal{K} - \mathcal{V} = \frac{Q^2}{2C} - \frac{\hbar^2}{8e^2L}\varphi^2 + E_J(V_g)\sqrt{2(1+\cos\varphi)}. \tag{4.15}$$

As usual, the resistance R causes dissipation to the environment, and therefore the term $\hbar\dot{\varphi}/2eR$ is left out of the Lagrangian formalism. The external I_{ext} is interpreted as the driving force and can be included into the potential of the Lagrangian in the form

$$\mathcal{V}_d = -\frac{\hbar}{2e}\varphi I_{ext}(t). \tag{4.16}$$

However, if $I_{ext}(t) = I_e \cos(\omega t)$, as is the case here, the average potential over time equals to zero.

4.2 Quantum Mechanical Model of the Circuit

The Lagrangian (4.15) with the drive potential can be used to derive the Hamiltonian of the system. Generally, the Hamilton's function of a physical system is defined as [20]

$$\mathcal{H} = \sum_i p_i \dot{q}_i - \mathcal{L}, \tag{4.17}$$

where the p_i's and $\dot{q}_i$'s are the generalized momenta and velocities, respectively. Accordingly, the Hamiltonian can also be written as a sum of the kinetic and the potential energies of the system. In this particular case, the Hamiltonian is therefore

$$\mathcal{H} = \frac{Q^2}{2C} + \frac{\hbar^2}{8e^2L}\varphi^2 - E_J(V_g)\sqrt{2(1+\cos\varphi)} - \frac{\hbar}{2e}\varphi I_{ext}(t). \tag{4.18}$$

The quantization of the charge and phase, done in Section (2.2.3), led to Equation (2.37). Because $\hbar\dot{\varphi}/2e = V = Q/C$, one gets by substituting that

$$\hat{\mathcal{H}} = -\frac{4e^2}{2C}\frac{\partial^2}{\partial\varphi^2} + \frac{\hbar^2}{8e^2L}\varphi^2 - E_J(V_g)\sqrt{2(1+\cos\varphi)} - \frac{\hbar}{2e}\varphi I_{ext}(t). \tag{4.19}$$

The transported charge is $2e$, and therefore the charging energy related to a single Cooper pair tunneling is denoted by $E_q = 4e^2/2C$. Then the effective *Hamilton's operator* of the system is

$$\hat{\mathcal{H}} = -E_q\frac{\partial^2}{\partial\varphi^2} + \frac{\hbar^2}{8e^2L}\varphi^2 - E_J(V_g)\sqrt{2(1+\cos\varphi)} - \frac{\hbar}{2e}\varphi I_{ext}(t). \tag{4.20}$$

The *Schrödinger* equation for a Hamiltonian is in general

$$\hat{\mathcal{H}}\Psi = \hat{E}\Psi, \tag{4.21}$$

and for the system at hand it is

$$\begin{aligned}\Big(&- E_q \frac{\partial^2}{\partial \varphi^2} + \frac{\hbar^2}{8e^2 L}\varphi^2 \\ &- E_J(V_g)\sqrt{2(1+\cos\varphi)} - \frac{\hbar}{2e}\varphi I_{ext}(t)\Big)\Psi = i\hbar\frac{\partial}{\partial t}\Psi.\end{aligned} \tag{4.22}$$

This implies that

$$\begin{aligned}\Big(&\frac{\partial^2}{\partial \varphi^2} - \frac{\hbar^2}{8e^2 L E_q}\varphi^2 + \frac{E_J(V_g)}{E_q}\sqrt{2(1+\cos\varphi)} \\ &+ \frac{\hbar}{2eE_q}\varphi I_{ext}(t) + \frac{i\hbar}{E_q}\frac{\partial}{\partial t}\Big)\Psi = 0.\end{aligned} \tag{4.23}$$

Here the E and the Ψ are the *eigenenergy* and the *eigenfunction* of the system, respectively.

Chapter 5

Simulations and Calculations

"In theory, there is no difference between theory and practice. But, in practice, there is."
- Jan L. A. van de Snepscheut

In this chapter some numerical results of the circuit presented above are discussed. The approximations made in the previous chapter are also used in the following. The parameters of the circuit are chosen to be the same as in the experiments made by the Helsinki group.

5.1 Reflection Coefficient

Let us feed a current I_{in} through the coupling capacitor C_c to the L-SET circuit. Because the impedances between the feedline and the circuit differ from each other, a part of the incoming current is reflected [53]. Both the incoming and the reflected current (I_{in} and I_r, respectively) can be measured and thereafter used in determining the *reflection coefficient*

$$\Gamma = \frac{I_r}{I_{in}}. \tag{5.1}$$

Naturally, one expects the reflection coefficient Γ to have values in the range of $[0, 1]$. Usually, when the probed system is linear, the reflection coefficient can be calculated as a function of the feedline impedance Z_0 and the system impedance Z [53]

$$\Gamma = \frac{Z - Z_0}{Z + Z_0}. \tag{5.2}$$

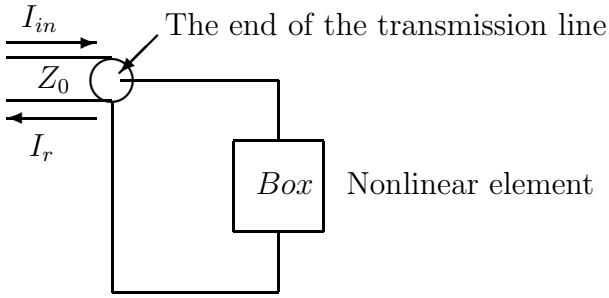

Figure 5.1: A transmission line terminated at L-SET system.

In this case, however, the system is *not* linear due to the nonlinear inductance of the two Josephson junctions. This makes the calculation of the reflection coefficient a little more complicated.

The circuit presented in Figure 4.1 can be studied as a transmission line that is terminated to impedance Z (see Figure 5.1). However, due to the nonlinearity of the L-SET system, the impedance is not well defined. Therefore the whole L-SET system is denoted only by Box. The travelling waves of the voltage V and the current I in the transmission line can be written in the form

$$\begin{aligned} V(x,\omega) &= V_- e^{\gamma x} + V_+ e^{-\gamma x} \\ I(x,\omega) &= -\frac{V_-}{Z_0} e^{\gamma x} + \frac{V_+}{Z_0} e^{-\gamma x}. \end{aligned} \tag{5.3}$$

Here the V_+ and V_- are the amplitudes of the incoming and the reflected waves, respectively. Both of the amplitudes are complex and depend on ω, which is the frequency of the input current. The quantity γ is called the propagation function and its form will be of no importance in here, as will be seen later. [53]

At the end of the line ($x = 0$) the travelling waves simplify to

$$\begin{aligned} V(0,\omega) \equiv V(\omega) &= V_- + V_+ \\ I(0,\omega) \equiv I(\omega) &= -\frac{V_-}{Z_0} + \frac{V_+}{Z_0}. \end{aligned} \tag{5.4}$$

This implies that

$$\begin{aligned} V_+ &= \frac{1}{2}\big(V(\omega) + Z_0 I(\omega)\big) \\ V_- &= \frac{1}{2}\big(V(\omega) - Z_0 I(\omega)\big). \end{aligned} \tag{5.5}$$

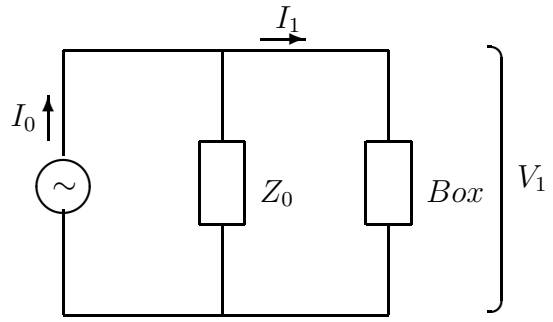

Figure 5.2: Equivalent circuit model for the probed L-SET system.

Here the V_+ is fixed by the incoming radiation. The reflection coefficient can now be expressed as

$$\Gamma = \frac{V_-}{V_+} = \frac{V(\omega) - Z_0 I(\omega)}{V(\omega) + Z_0 I(\omega)}. \tag{5.6}$$

The actual numerical calculation of reflection coefficient in Equation (5.6) is somewhat difficult due to the nonlinearity of the system.

On the other hand, let us consider a circuit depicted in Figure 5.2. Now the Box is connected parallel with the feedline impedance Z_0 and a current is fed to this system by a current source I_0. The potential difference accross the Box is simply $V_1 = Z_0(I_0 - I_1)$ which implies

$$V_1 + Z_0 I_1 = Z_0 I_0. \tag{5.7}$$

Now, if one identifies V with V_1 and I with I_1 one sees that solving the reflection coefficient of the circuit in Figure 5.1 is equivalent to solving the circuit in Figure 5.2 numerically. That is why the circuit above is called as the *equivalent circuit model* for the probed L-SET system. This way $2V_+ = Z_0 I_0$, $2V_- = Z_0 I_0 - 2Z_0 I_1$ and the reflection coefficient reduces to

$$\Gamma = \frac{I_0 - 2I_1}{I_0}. \tag{5.8}$$

The equivalent circuit is numerically solved in the following subsection.

5.1.1 Equation of Motion

The derivation of the equation of motion of the equivalent circuit model is begun, as in the previous chapter, with the Kirchhoff loop rules. The input

current I_0 equals to the sum of I_{Z_0} and I_1 that are the currents through the impedance Z_0 and the *Box*, respectively. That is,

$$I_0 = I_{Z_0} + I_1. \tag{5.9}$$

Let us first consider a case where the coupling capacitance is equal to zero, i.e. $C_c = 0$. In this way, $I_1 = I_{ext}(t)$ and the total input current can be written as

$$I_0 = \frac{\hbar}{2eZ_0}\dot{\varphi} + C\frac{\hbar}{2e}\ddot{\varphi} + \frac{\hbar}{2eR}\dot{\varphi} + \frac{\hbar}{2eL}\varphi + \frac{2e}{\hbar}E_J(V_g)\frac{\sin\varphi}{\sqrt{2(1+\cos\varphi)}}. \tag{5.10}$$

This can be again written in a dimensionless form

$$\frac{I_0}{I_c} = \frac{d^2\varphi}{d\tau^2} + \frac{\hbar\omega_p}{2eI_c}\left(\frac{1}{Z_0} + \frac{1}{R}\right)\frac{d\varphi}{d\tau} + \frac{\hbar}{2eLI_c}\varphi + \frac{\sin\varphi}{\sqrt{2(1+\cos\varphi)}}, \tag{5.11}$$

which implies

$$\begin{aligned}\frac{d^2\varphi}{d\tau^2} &= \frac{I_0}{I_c} - \frac{\hbar\omega_p}{2eI_c}\left(\frac{1}{Z_0} + \frac{1}{R}\right)\frac{d\varphi}{d\tau} - \frac{\hbar}{2eLI_c}\varphi - \frac{\sin\varphi}{\sqrt{2(1+\cos\varphi)}} \\ &\equiv f(\tau, \varphi, \dot{\varphi}),\end{aligned} \tag{5.12}$$

where the derivation with respect to τ is denoted also by a dot. By denoting $\chi = \dot{\varphi}$ one gets a pair of coupled first order differential equations

$$\begin{cases} \dot{\chi} = f(\tau, \varphi, \chi) \\ \dot{\varphi} = \chi(\tau, \varphi, \chi) \end{cases} \tag{5.13}$$

which can be solved numerically by the fourth order Runge-Kutta method [54]. This, however, does not describe the circuit at hand and one has to pay attention also to the effects of the coupling capacitor C_c.

If the coupling capacitance is taken into consideration, the situation becomes somewhat more complicated, as can be seen in Figure 5.3. Namely, again with the help of the Kirchhoff rules, a pair of equations can be formed

$$V_1 + \frac{1}{C_c}\int I_1 dt = Z_0(I_0 - I_1) \tag{5.14}$$

$$I_1 = I_{ext}(t). \tag{5.15}$$

By taking the derivative of the Equation (5.14) with respect to time, one obtains

$$\dot{I}_1 = \dot{I}_0 - \frac{1}{Z_0 C_c}I_1 - \frac{\dot{V}_1}{Z_0}. \tag{5.16}$$

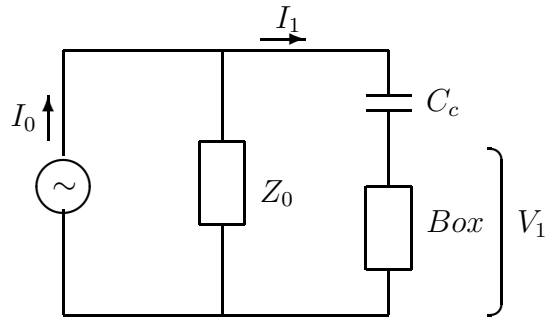

Figure 5.3: Equivalent circuit model for the probed L-SET system with coupling capacitor.

This can again be changed to dimensionless variables, and by denoting the derivative with respect to τ with a dot, one obtains

$$\frac{\dot{I}_1}{I_c} = \frac{\dot{I}_0}{I_c} - \frac{1}{Z_0\omega_p C_c}\frac{I_1}{I_c} - \frac{1}{CZ_0\omega_p}\ddot{\varphi} \equiv f_1(\tau, \ddot{\varphi}, I_1). \tag{5.17}$$

Also,

$$\ddot{\varphi} = \frac{I_1}{I_c} - \frac{\hbar\omega_p}{2eI_cR}\dot{\varphi} - \frac{\hbar}{2eLI_c}\varphi - \frac{\sin\varphi}{\sqrt{2(1+\cos\varphi)}} \equiv f_2(\tau, \varphi, \dot{\varphi}, I_1) \tag{5.18}$$

Now, one actually notices that $\ddot{\varphi}$ dependence in the function $f_1(\tau, \ddot{\varphi}, I_1)$ can be eliminated. By doing so, one obtains $f_1(\tau, \ddot{\varphi}, I_1) \equiv f_1(\tau, \varphi, \chi, I_1)$, where it has been denoted that $\chi = \dot{\varphi}$. This way, one obtains a group of coupled first order differential equations

$$\begin{cases} \dot{I}_1 = f_1(\tau, \varphi, \chi, I_1) \\ \dot{\chi} = f_2(\tau, \varphi, \chi, I_1) \\ \dot{\varphi} = \chi(\tau, \varphi, \chi, I_1)) \end{cases} \tag{5.19}$$

This group can also be solved by fourth order Runge-Kutta method for systems of differential equations [54].

5.2 System Parameters and Results

The parameters used for the computation were the same that have been obtained from the measurements in Helsinki. The calculations were made for two

Sample	R_{SSET} (kΩ)	E_J (K)	E_c (K)	L (nH)	C (pF)	C_c (pF)
1	4.2	3.5	0.17	3	23	0.72
2	9.6	1.6	0.92	7.4	8.4	0.72

Table 5.1: Parameters of the two samples measured in Helsinki.

samples one of which was purely classical, i.e. $E_J \gg E_c$. The other one had the Josephson energy $E_J \gtrsim E_c$ and was expected to undergo reduced SSET processes (above all to have the gate charge dependent critical current). The parameters of the two samples are shown in Table 5.1. The inductance and capacitance of the LC-oscillator were determined by measuring the resonance frequency at $T = 4$ K with known components. Also, if one considers the junctions composing the SSET to be identical, then the single-junction tunneling resistance R_T is half of the SSET resistance. This is, of course, of no importance when the quasiparticle tunneling is neglected, as is the case in here. However, with the help of R_T and the approximated value of the superconducting gap Δ one is able to obtain the single-junction value for the E_J. The capacitive energy of the whole SSET is approximated by the experimenters. Their quess is based on experience and the symmetry of the SSET.

In the spirit of Subsection 3.4.2 one is able to approximate the supercurrent through two junction SSET. When the individual Josephson energies of the two junctions are E_J the Josephson energy $E_{J,SSET} \equiv E_J(V_g)$ of the approximation can have values $0 < E_J(V_g) < E_J$, depending on the gate voltage V_g. Let us take this into consideration by denoting $E_J(V_g) \equiv \beta(V_g)E_J$ where $\beta(V_g) \in (0, 1)$. When the junction is classical, as is the case with Sample 1, β can be taken as constant 1. This means naturally, that the gate voltage does not affect to the supercurrent through the SSET.

The potential energies according to Equation (4.12) are shown in Figure 5.4, corresponding to the parameter values given in Table 5.1 for the two samples. The local minima of this potential are found by derivating it with respect to φ and by setting this derivative to zero

$$\frac{d\mathcal{V}}{d\varphi} = \frac{\hbar^2}{4e^2L}\varphi + E_J(V_g)\frac{\sin\varphi}{\sqrt{2(1+\cos\varphi)}} = 0. \tag{5.20}$$

This equation can be simplified for the calculations into form

$$f(\varphi) = \varphi + \gamma\frac{\sin\varphi}{\sqrt{2(1+\cos\varphi)}} = 0, \tag{5.21}$$

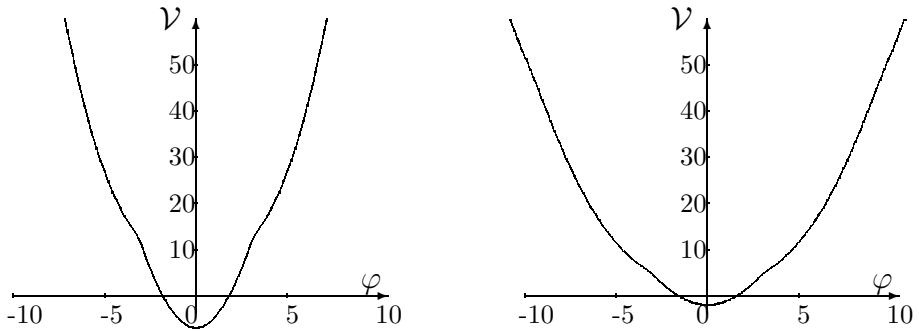

Figure 5.4: Potential energy of the system for the Samples 1 (left) and 2 (right). The relevant energies are measured in Kelvin's.

where $\gamma = E_J(V_g)4e^2L/\hbar^2$. This was again derivated with respect to φ and the minima were looked for. The first positive minimum sets a lower bound for γ which was found to be $\gamma > \pi$. This means that when the ratio $E_J(V_g)4e^2L/\hbar^2$ exceeds π, one is expected to find a minimum in the potential $\mathcal{V}$, other than $\varphi = 0$. However, with the parameter values used here one obtains

$$E_J(V_g)4e^2L/\hbar^2 \ll \pi. \tag{5.22}$$

So, no potential minima (other than $\varphi = 0$) is found in the present approximation.

One is also able to calculate the asymptotic behaviour of the resonance frequency. According to Equation (4.9) one gets that

$$f_0 = \frac{\omega_0}{2\pi}$$
$$f_r = \frac{1}{2\pi}\sqrt{\omega_0^2 + \frac{\omega_p^2}{2}}.$$

For Sample 1 $\beta(V_g) \approx 1$ and one gets that $f_0 = 606$ MHz and $f_r = 784$ MHz. For Sample 2 let us approximate $\beta(V_g) \approx 0.65$, which leads to $f_0 = 638$ MHz and $f_r = 847$ MHz. These are, nevertheless, not the true values of the f_0 and f_r due to the effects caused by the coupling capacitance. The more realistic values are seen in the simulations made in the following subsection. Based on the discussion above in this chapter, one expects a shift from f_r to f_0 when the fluctuations of the phase φ get bigger, i.e. the drive current is increased. This shift has been seen both in experiments and simulations.

5.2.1 Resonance Frequency Shift

The shift in the resonance frequency can be measured in the following way. An alternating current $I_0 = I_e \cos(\omega t)$ is called *carrier current* and fed to the resonator (LC + SSET) via the feedline with impedance $Z_0 = 50\ \Omega$. On the boundary between the feedline and the resonator, part of the incoming current is reflected and the rest is transmitted to the resonator. The argument and the magnitude of the complex reflection coefficient can both be measured by a proper network analyzer. This measurement has actually been done by M. Sillanpää et al. A theoretical simulation of the situation is presented here.

The reflection coefficient is determined numerically in the following way. At first, one solves the current I_1 as a function of time according to the group of linear equations (5.19). Simultaneously, its (complex) Fourier component $I_1(f)$ corresponding to the carrier frequency $f = \omega/2\pi$ is calculated. Then one is able to calculate the reflection coefficient according to Equation (5.8). This calculation is repeated with different values of carrier amplitude and frequency.

The results of the simulations of the Sample 1 are shown in Figure 5.5. On the left is the contour plot of the magnitude $|\Gamma|$ of the current reflection coefficient $\Gamma = |\Gamma| e^{i \arg(\Gamma)}$ as a function of frequency and power of the incoming current. The power is measured in decibels according to

$$dB = 10 \cdot \log_{10}(P_1/P_0), \tag{5.23}$$

where P_1 is the incoming power and P_0 the reference power. Here P_0 is set to 1 mW, which leads to power unit dB**m**. Because the incoming voltage can be written as $V_+ = Z_0 I_e/2$, the incoming power P_1 can be calculated by using relation [14]

$$P_1 = \frac{V_+^2}{2Z_0} = \frac{Z_0 I_e^2}{8}. \tag{5.24}$$

From the left hand side contour plot, one sees clearly the shift in resonance frequency at the *critical power* $P_c \approx -100$ dBm. A same kind of plotting of the argument of Γ has been done on the right hand side of Figure 5.5. A similar kind of behaviour has also been detected in classical junctions by I. Siddiqi et al. in Yale [55].

In the simulations the magnitude got values from 0.83 (black) to 1.00 (white). Similarly, the argument had values from 0.04 (black) to 0.26 (white). When results obtained for the magnitude are compared to the measured data (see Figure 5.6), one sees that the width of the resonance peaks as well as

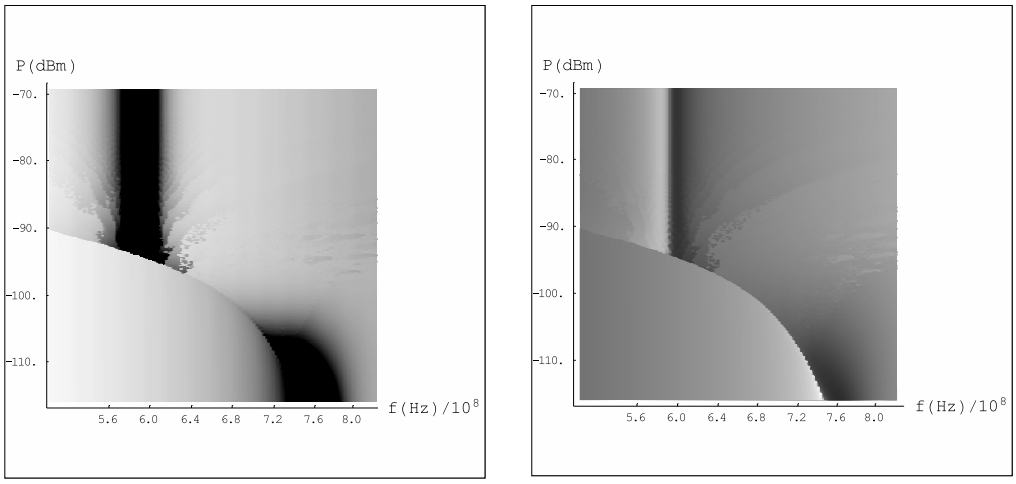

Figure 5.5: Depedence of the calculated reflection coefficient Γ on the frequency f and the amplitude I_e of the incoming current I for Sample 1. On the left is the contour plot of the magnitude of Γ. The gray-scale goes from 0.83 (black) to 1.00 (white). On the right is the countour plot of the argument of Γ with the gray-scale from 0.04 (black) to 0.26 (white).

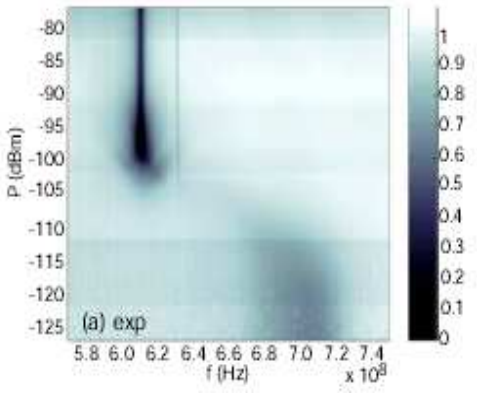

Figure 5.6: Measured magnitude of the reflection coefficient for Sample 1.

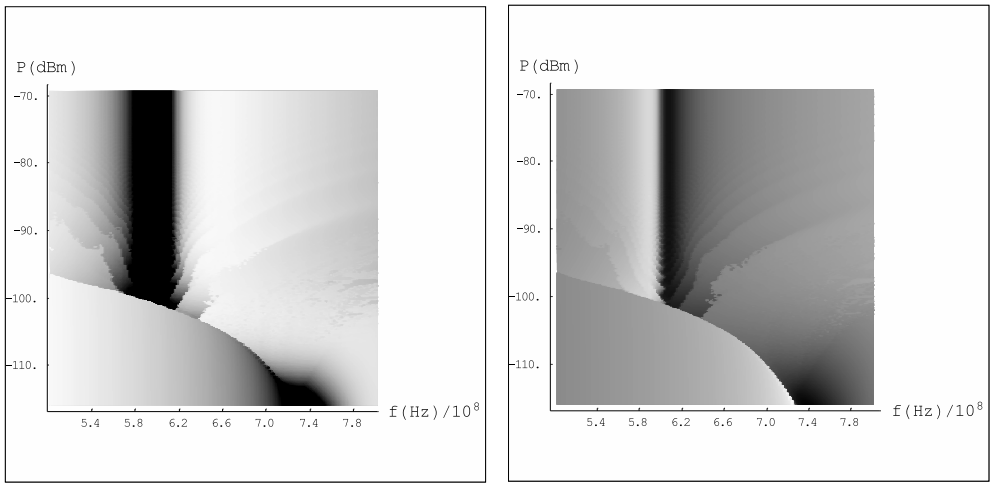

Figure 5.7: Simulated reflection coefficient for Sample 1 with $C = 25$ pF, $L = 2.76$ nH and $C_c = 1.76$ pF. The gray-scale runs from 0.51 (black) to 0.96 (white) for the magnitude and from -0.13 (black) to 0.61 (white) for the argument. Notice that the scales differ from those in Figure 5.5.

the asymptotic resonance frequencies are larger in the simulations than in the physical system. Moreover, the depths of the resonance peaks are smaller in the simulations. However, this does not present a problem, because by changing the parameter values one is able to alter these properties to the right direction. The changes are well justified up to a certain limit because there always exists some error when these kind of parameters are measured. So, in Figure 5.7 one sees the effects of slightly adjusted parameter values. The anticipated shift in the resonance frequency can be seen in the Figures at the critical power $P_c \approx -100$ dBm. Also, the simulated amplitude of the reflection coefficient agrees qualitatively well with the measured one.

The simulations show that the effects of changing the parameter values are as follows. A growth in the capacitance C increases the gap between the two resonance peaks. It also results in lower resonance peaks. Moreover, if one increases the inductance L, both of the peaks are shifted to smaller frequencies by an equal amount. Also, the peaks are lowered. Similarly, the bigger is the resistance R, the lower are the resonance peaks. The growing of the coupling capacitance, however, leads to higher resonance peaks. It also shifts the peaks to lower frequencies and lowers the critical power. In addition, if one reduces the Josephson energy E_J one obtains higher and narrower peaks.

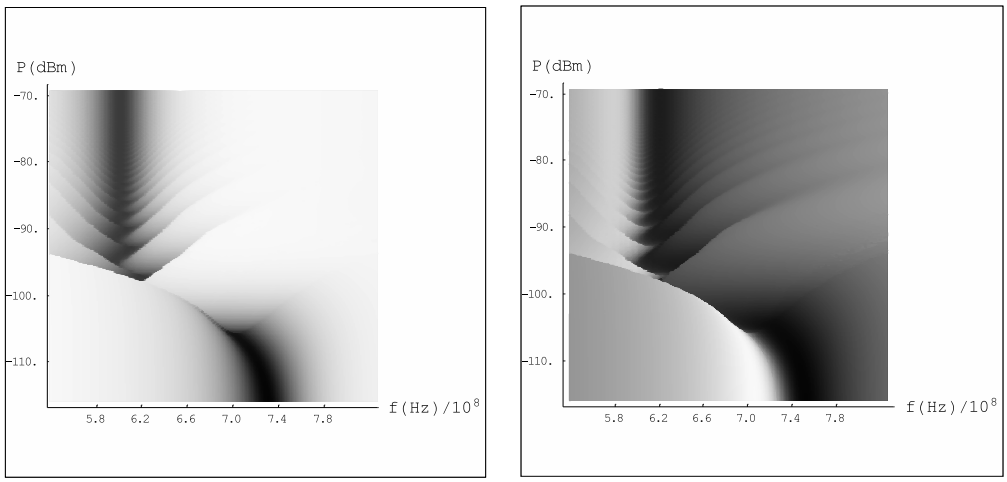

Figure 5.8: Simulated magnitude (left) and argument (right) of the reflection coefficient for Sample 2. The gray-scale for the magnitude plot runs from 0.54 (black) to 0.97 (white). For the argument plot the scale goes from -0.08 (black) to 0.48 (white).

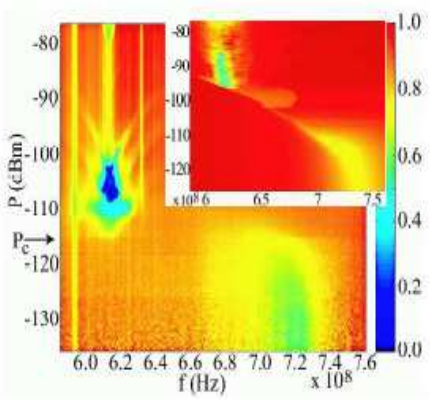

Figure 5.9: Measured magnitude of the reflection coefficient for Sample 2. The inset shows the results obtained in Helsinki with the Aplac circuit simulator.

When the same kind of calculations are applied to the parameters of the Sample 2, the results look like Figure 5.8. The color scale for the magnitude runs from 0.54 (black) to 0.97 (white) and for the argument from -0.08 (black) to 0.48 (white). Again, the simulations can be compared with the measurements. In Figure 5.9 one sees the measured magnitude of the reflection coefficient obtained in Helsinki [49, 50]. When one examines the plot of Sample 2 one sees an interesting "hair"-like structure in the regime of high input power. It is related to the resistance R. Namely, when R is small the hairs are longer and vice versa. All in all, the simulations show for both samples the anticipated resonance frequency shifts at the critical power and are also in other respects in qualitatively good correspondence with the measurements. However, there exist also some differences between the simulated and the measured data. The "satellite dips" on both sides of the resonance peak at f_0 are not seen in the simulations. Moreover, the depth of the resonance peak is constant in simulations with all power values. In the measurements the peak is lower at small input powers than at high ones. Also, the measured resonance frequency shift is discrete for Sample 2 even though it is clearly continuous in simulations.

5.2.2 Effect of the Gate Capacitance

If one wishes to use the L-SET circuit as a charge detector, it is important that the change in gate charge Q_g has some effect in the reflected current. Because in the weak coupling regime the supercurrent through the L-SET is dependent on the gate charge, this effect could be expected in the Sample 2. As explained before, the effects of the gate charge to the Josephson energy $E_J(V_g)$ of the two junction system can be taken into account by introducing the factor $\beta(V_g)$, so that $E_J(V_g) = \beta(V_g)E_J$. Here the E_J is the single junction Josephson energy. The exact form of the factor $\beta(V_g)$ is not derived here, but the simulations are performed with linearly spaced $\beta(V_g)$ values. So, the effect of gate voltage is seen by plotting the magnitude and the argument of the reflection coefficient as a function of incoming frequency ω with different values of $\beta(V_g)$. The results are shown in Figure 5.10. The depenedence of both, magnitude and argument, on the fluctuations in the gate voltage can clearly be seen. This way one gets information of the gate charge by measuring the magnitude or the argument of the reflection coefficient. However, due to the lack of the exact form of the $\beta(V_g)$, one is not able to the tell details about the sensitivity of the device.

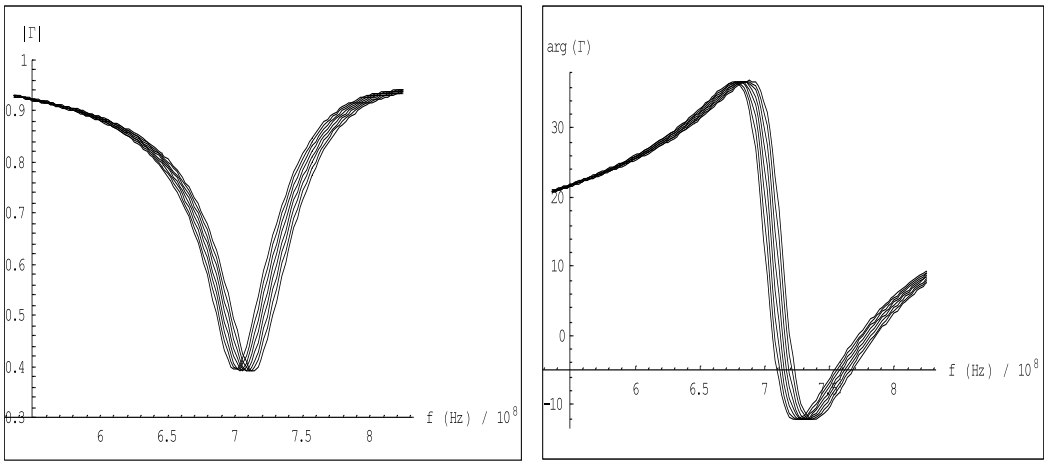

Figure 5.10: The magnitude (left) and the argument (right) of the reflection coefficient Γ of Sample 2 drawn as a function of f with different values of $\beta(V_g)$.

5.3 Discussion

"I have not failed. I have found 10.000 ways that do not work."
-Benjamin Franklin

Based on the simulations made, it is obvious that the simple model derived for the reflection coefficient is qualitatively in good agreement with the real physical quantity. The dynamics of both, the magnitude and the argument, were similar to those obtained from the experiments. Also, the dependence of both of them on the gate charge was shown in the simulations. Therefore, it is possible to measure the charge on the gate capacitor by measuring the magnitude or the argument of the reflection coefficient. Because one is able to measure them with extreme precision, one is therefore capable of measuring the gate charge with similar accuracy. This way one might be able to build very precise charge detectors using the inductive SSET structure presented here.

The main defect in the model is the lack of correct way of the approximating the effects of the gate voltage to the potential energy. The potential was approximated quite brutally by connecting the two asymptotic limits in a very simple way. The calculation of the correct potential would probably lead

to better correspondence with the reality and should tell something about the sensitivity of the device. All in all, the next steps should also include the solving of the Schrödinger equation (4.23) and thereafter trying to find the causes of the properties that were not discovered here. A similar kind of theoretical results have also been obtained from Harmonic Balance simulations done with Aplac circuit simulator by M. Sillanpää et al. [49, 50].

It is worthwhile also to mention, that the inductive SSET can be used in the redefinition of the present current standard. Namely, nowadays the definition of ampere needs a concept of an infinitely long wire, and therefore is not practical for the realization of the unit of current. However, with the help of single electron tunneling this problem could be circumvented [56].

Chapter 6

Conclusions

> *"There is a theory which states that if ever anybody discovers exactly what the Universe is for and why it is here, it will instantly disappear and be replaced by something even more bizarre and inexplicable. There is another theory which states that this has already happened."*
> -Douglas Adams

The purpose of this thesis was to present a new kind of way to measure charge. It was done by introducing a device whose operational principle was similar to the present state-of-the-art charge detector, RF-SET. The gadget was called as the inductive superconducting SET. The illustration was started with the fundamentals of the tunnel junctions and Josephson junctions. Thereafter, a peak to the tunneling rates of a single junction was made. After that, the structure of an ordinary SET was presented and theory was then developed to cover also the SETs that are in the superconducting state. A short introduction to quantum computing was also made to get some motivation for the following treatments.

After this introductory part, the model of the new circuit was presented. The system was handled both classically and quantum mechanically. Equivalent circuit model of the system was formed before the numerical calculations were made. The coupled linear first order differential equations were solved with fourth order Runge-Kutta method. The reflection coefficient of the system was determined by counting the Fourier component of the incoming current at carrier frequency. The results of the simulations were compared with the measurements and a qualitative correspondence was found. Also, the resonance

frequency was found to be dependent on the gate charge in the weak coupling regime, which is an essential feature if one wants to use the system in charge measurements. The possible corrections to the model and future prospects were discussed in the end.

In summary, a theory concerning the L-SET circuit has been presented. Also, probable applications have been proposed. The theory has been put into a test by simulating the reflection coefficient and comparing the results with the measured ones. Even though the correspondence between the theory and the measurements was quite good one should, however, not praise the theory as the gospel truth, but merely as an explanation.

"That's all I have to say about that."
- Forrest Gump

Bibliography

[1] R. P. Feynman, *The Feynman Lectures on Physics*, Vol. 3 (Addison-Wesley, USA, 1966).

[2] *Highest Critical Temperature Superconductor*, ed. G. Elert, http://hypertextbook.com/facts/2002/MichaelNg.shtml.

[3] M. Tinkham, *Introduction to Superconductivity* (McGraw-Hill, Inc., USA, 1996).

[4] R. Escudero, *The Superconducting Ceramics of High Transition Temperature (Basic Phenomena)*, http://www.materia.coppe.ufrj.br/sarra/artigos/artigo10114.

[5] E. Thuneberg, *Suprajohtavuus*, http://cc.oulu.fi/∼tf/tiedostot/pub/suprajohtavuus/luennot/supramon.pdf.

[6] V. L. Ginzburg and L. D. Landau, Zh. Eksp. Teor. Fiz. **20**, 1064 (1950). (The English translation in: L. D. Landau, *Collected papers of L. D. Landau* (Pergamon Press, Oxford, 1965) pp. 546.)

[7] J. Bardeen, L. N. Cooper and J. R. Schrieffer, Phys. Rev. **108**, 1175 (1957).

[8] B. D. Josephson, Phys. Lett. **1**, 251 (1962).

[9] P. W. Anderson and J. M. Rowell, Phys. Rev. Lett. **10**, 230 (1963).

[10] I. K. Yanson et al., Sov. Phys. JETP **21**, 650 (1965).

[11] T. P. Orlando et al., Phys. Rev. B **60**, 15398 (1999).

[12] C. H. van der Wal et al., Science **290**, 773 (2000).

[13] D. Deutsch, *Todellisuuden rakenne* (Terra Cognita, Helsinki, 1997).

[14] In any basic electromagnetism book, for example in I. S. Grant and W. R. Phillips, *Electromagnetism* (John Wiley and Sons Ltd., Manchester, 1990).

[15] T. Henning, arXiv:cond-mat/9710037 (1997).

[16] V. Z. Kresin and S. A. Wolf, *Fundamentals of Superconductivity* (Plenum Press, New York, 1990).

[17] G.-L. Ingold and Yu. V. Nazarov, in *Single Charge Tunneling*, edited by H. Grabert and M. H. Devoret (Plenum Press, New York, 1992) pp. 21-106.

[18] W. C. Stewart, Appl. Phys. Lett. **12**, 277 (1968).

[19] D. E. McCumber, J. Appl. Phys. **39**, 3113 (1968).

[20] L. D. Landau and E. M. Lifshitz, *Mechanics* (Butterworth-Heinemann, Oxford, 1981).

[21] M. Iansiti et al., Phys. Rev. B **39**, 6465 (1989).

[22] K. K. Likharev and A. B. Zorin, J. Low Temp. Phys. **59**, 347 (1985).

[23] H. Goldstein, *Classical Mechanics* (Addison-Wesley Publishing Company, Inc., USA, 1980).

[24] M. P. Marder, *Condensed Matter Physics* (John Wiley & Sons, Inc., USA, 2000).

[25] U. Geigenmüller and G. Schön, Phys. B **152**, 186 (1988).

[26] D. B. Haviland et al., Z. Phys. B **85**, 339 (1991).

[27] A. I. Larkin, K. K. Likharev and Yu. N. Ovchinnikov, Physica **126B+C**, 414 (1984).

[28] L. S. Kuzmin et al., Phys. Rev. B **54**, 14 (1996).

[29] A. D. Zaikin and D. S. Golubev, Phys. Lett. A **164**, 337 (1992).

[30] H. Seppä and J. Hassel, arXiv:cond-mat/0305263 (2003).

[31] J. Delahaye et al., Science **299**, 1045 (2003).

[32] G. Falci, V. Bubanja and G. Schön, Z. Phys. B **85**, 451 (1991)

[33] H. Grabert, Z. Phys. B **85**, 319 (1991).

[34] A. O. Caldeira and A. J. Leggett, Ann. Phys. (N. Y.) **149**, 374 (1983).

[35] A. O. Caldeira and A. J. Leggett, Phys. Rev. Lett. **46**, 211 (1981).

[36] J. J. Sakurai, *Advanced Quantum Mechanics* (Addison-Wesley, USA, 1985).

[37] G. Baym, *Lectures on Quantum Mechanics* (The Benjamin/Cummings Publishing Company, USA, 1973) pp. 134-136.

[38] I. Giaever, Phys. Rev. Lett. **5**, 147 (1960).

[39] I. Giaever, Phys. Rev. Lett. **5**, 464 (1960).

[40] J. Nicol, S. Shapiro and P. H. Smith, Phys. Rev. Lett **5**, 461 (1960).

[41] M. H. Devoret et al., Phys. Rev. Lett. **64**, 1824(1990).

[42] T. A. Fulton and G. J. Dolan, Phys. Rev. Lett. **59**, 109 (1987).

[43] M. van der Brink et al., Z. Phys. B - Condensed Matter **85**, 459 (1991).

[44] D. V. Averin and Yu. V. Nazarov, Phys. Rev. Lett. **69**, 1993 (1992).

[45] M. T. Tuominen et al., Phys. Rev. Lett. **69**, 1997 (1992).

[46] A. J. Leggett, Science **296**, 861 (2002).

[47] C. Cohen-Tannoudji, B. Diu and F. Laloë, *Quantum Mechanics* (Wiley, New York, 1977, vol. 1, pp. 405-415).

[48] J. Brown, *Kvanttitietokone* (Terra Cognita, Helsinki, 2000).

[49] M. Sillanpää et al., arXiv:cond-mat/0402045 (2004).

[50] M. Sillanpää et al., *Dynamics of the Inductive Single-Electron Transistor*, not yet published.

[51] A. B. Zorin, Phys. Rev. Lett. **76**, 4408 (1996).

[52] A. B. Zorin, Phys. Rev. Lett. **86**, 3388 (2001).

[53] W. R. LePage and S. Seely, *General Network Analysis* (McGraw-Hill Book Company, Inc., USA, 1952).

[54] *Handbook of Mathematical Functions*, eds. M. Abramowits and I. A. Stegun (U.S. Goverment Printing Office, Washington, D. C., 1972).

[55] I. Siddiqi et al., arXiv:cond-mat/0312553 (2003).

[56] A. B. Zorin et al., *Metrology Based on Single Charge Quantum Devices: Towards The Quantum Standard Of Current*, http://www-lpm2c.grenoble.cnrs.fr/nanosciences/CIRP/zorin.pdf